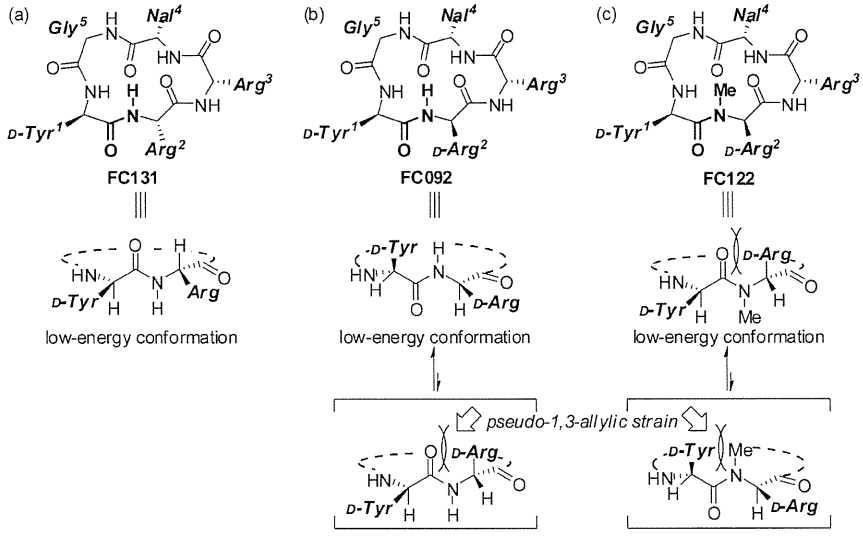


**Figure 1.** Structures of cyclic pentapeptide CXCR4 antagonists and the bioactivity-relevant peptide bond orientations in D-Tyr-L-Arg in FC131 (a), D-Tyr-D-Arg in FC092 (b), and D-Tyr-D-MeArg in FC122 (c). Nal = L-3-(2-naphthyl)alanine.

the D-Tyr[1]-Arg[2] substructure using a series of alkene dipeptide isosteres. Computational analysis was also performed to assess the binding mode to CXCR4 of FC131 and its derivatives.

## RESULTS AND DISCUSSION

**Design and Synthesis of a Series of FC131 Derivatives Containing Alkene Dipeptide Isosteres.** Peptide bonds constitute the assembly units for secondary and tertiary structures as well as the functional motifs for intermolecular interactions with binding partners via hydrogen bond acceptor/donor properties. Because replacement of peptide bonds with isosteric mimetics is one of the usual practices in performing SAR studies on bioactive and functional peptides, a number of peptide bond isosteres have been developed and used in medicinal chemistry. To identify the dominant conformations that contribute to the bioactivity of FC131 derivatives, alkene dipeptide isosteres were used for the SAR study (Figure 2). A planar alkene motif can restrict the possible *cis*/*trans* isomerization of peptide bonds.[23−25] In the trisubstituted alkene isosteres,[26,27] a $\gamma$-methyl group serves as a substituent corresponding to the carbonyl oxygen of a peptide bond. Tetrasubstituted alkene isosteres mimic *N*-methylamide bonds.[28] Our expectation was that, using a series of alkene isosteres, the steric effects of the carbonyl group and *N*-methyl group of the D-Tyr−Arg peptide bond on the peptide conformation and bioactivity could be understood. The contributions of the D-Tyr−Arg peptide bond to the hydrogen-bonding interactions could also be revealed by replacement with the isosteres because these substituted alkene motifs cannot engage in dipole interactions (Figure 3).

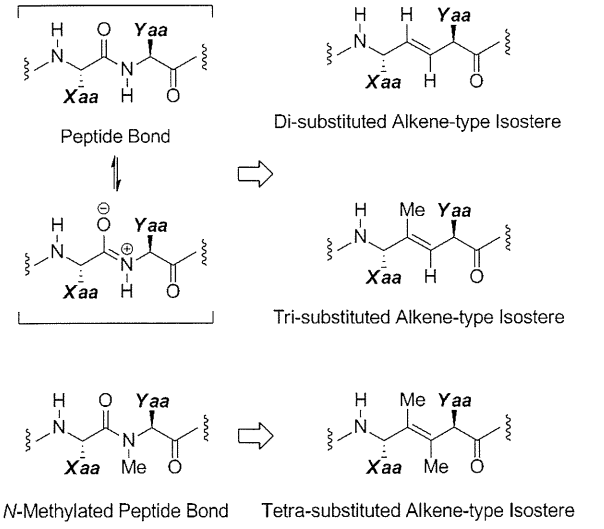


**Figure 2.** Structures of a series of alkene dipeptide isosteres. Xaa and Yaa = amino acid side chains.

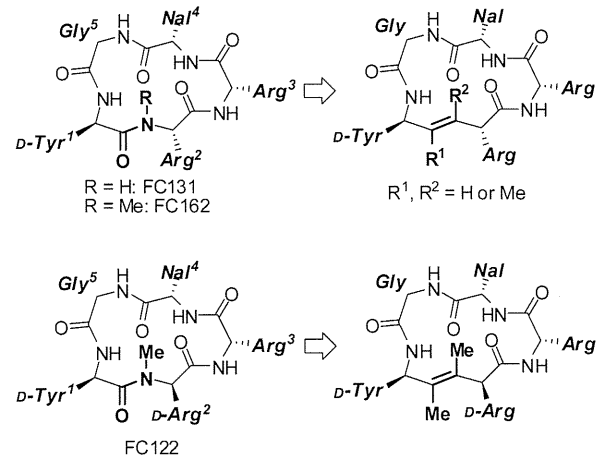


**Figure 3.** Design of alkene isostere-containing derivatives of cyclic pentapeptide-based CXCR4 antagonists. Nal = L-3-(2-naphthyl)-alanine.

For the coupling component in the solid-phase peptide synthesis, a fully protected D-Tyr-Orn isostere, **10** (Orn = L-ornithine), was designed in which the Orn $\delta$-amino group can be converted into an Arg guanidino group after peptide synthesis.[29,30] A synthetic method for disubstituted alkene dipeptide isosteres has previously been reported.[31] Initially, the D-tyrosine derivative **1** was converted to *syn*-allyl alcohol **2** by a one-pot reduction and vinylation (Scheme 1). After protection of the hydroxyl group of **2** with an acetyl group, ozonolysis and


dx.doi.org/10.1021/jm2016914 | J. Med. Chem. 2012, 55, 2746−2757

**Scheme 1**[a]

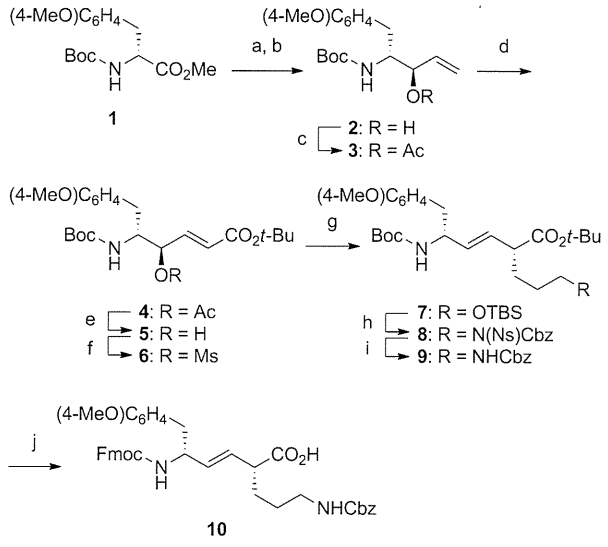


[a]Reagents and conditions: (a) DIBAL-H, $CH_2Cl_2$–toluene, −78 °C, 20 min, then $H_2C$=CHMgBr, $ZnCl_2$, LiCl, THF, −78 °C, 3 h (31%); (b) recrystallization; (c) $Ac_2O$, pyridine, DMAP, $CHCl_3$, 0 °C, 2 h (quantitative); (d) (i) $O_3$, EtOAc, −78 °C, then $Me_2S$, 0 °C, 30 min; (ii) $(EtO)_2P(O)CH_2CO_2$-*t*-Bu, LiCl, $(i\text{-}Pr)_2NEt$, MeCN, 0 °C, 3 h (62%); (e) $K_2CO_3$, MeOH, rt, 2 h (96%); (f) MsCl, $Et_3N$, $CH_2Cl_2$, 0 °C, 2 h (96%); (g) TBSO$(CH_2)_3$Li, CuCN, LiCl, THF–$Et_2O$–*n*-pentane, −78 °C, 30 min (94%); (h) (i) $H_2SiF_6$(aq), MeCN–$H_2O$, rt, 2 h; (ii) NsNH(Cbz), DEAD, $PPh_3$, THF–toluene, 0 °C, 3 h (86%); (i) PhSH, $K_2CO_3$, DMF, rt, 3 h (96%); (j) (i) TFA, $CH_2Cl_2$, rt, 2 h; (ii) FmocOSu, $Et_3N$, MeCN–$H_2O$, rt, 2 h (71%).

a subsequent Horner–Wadsworth–Emmons reaction (HWE reaction) afforded an (*E*)-isomer of *α,β*-enoate **4**. Alcoholysis of the acetyl group followed by mesylation yielded *γ*-(mesyloxy)-*α,β*-enoate **6**, which is a key substrate for organocopper-mediated $S_N2'$ alkylations. Treatment of **6** with TBSO$(CH_2)_3$Li in the presence of CuCN and LiCl gave an *α*-alkylated product, **7**. The side chain silyl ether group in **7** was converted to a Cbz-protected amino group via a Mitsunobu reaction using NsNH(Cbz). Removal of Ns, Boc and *t*-Bu groups, followed by *N*-Fmoc protection, provided the expected isostere component **10**.

Tri- and tetrasubstituted alkene isosteres for D-Tyr-Orn dipeptide were synthesized according to the protocol established in our previous studies.[32,33] *syn*-Allyl alcohols **12a,b** were obtained by sequential methylation and alkenylation of Weinreb amide **11** using Grignard reagents (Scheme 2). Cyclization of **12a,b** under basic conditions followed by Boc protection gave oxazolidinones **13a,b**. 5-Vinyloxazolidinone **13a** was converted to an *α,β*-unsaturated ester, **15a**, by ozonolysis and HWE reaction. In contrast, the same HWE reaction of ketone **14**, which was derived from 5-propenyloxazolidinone **13b**, did not proceed. The *β*-methylated congener **15b** was provided via Wittig reaction of **14** using $Ph_3P$=$CHCO_2$-*t*-Bu. Organocopper-mediated alkylations of **15a,b** gave the *anti*-$S_N2'$ products **16a,b** with moderate (*E*)-selectivity. Although the (*E*)- and (*Z*)-isomers of **16a** were not separated in this step, the (*E*)-isomer of alcohol **17a** was isolated by column chromatography. Alcohols **17a,b** were converted to the desired Fmoc-protected amino acids **20a,b** using methods identical to those described for the synthesis of **10**.

**Scheme 2**[a]

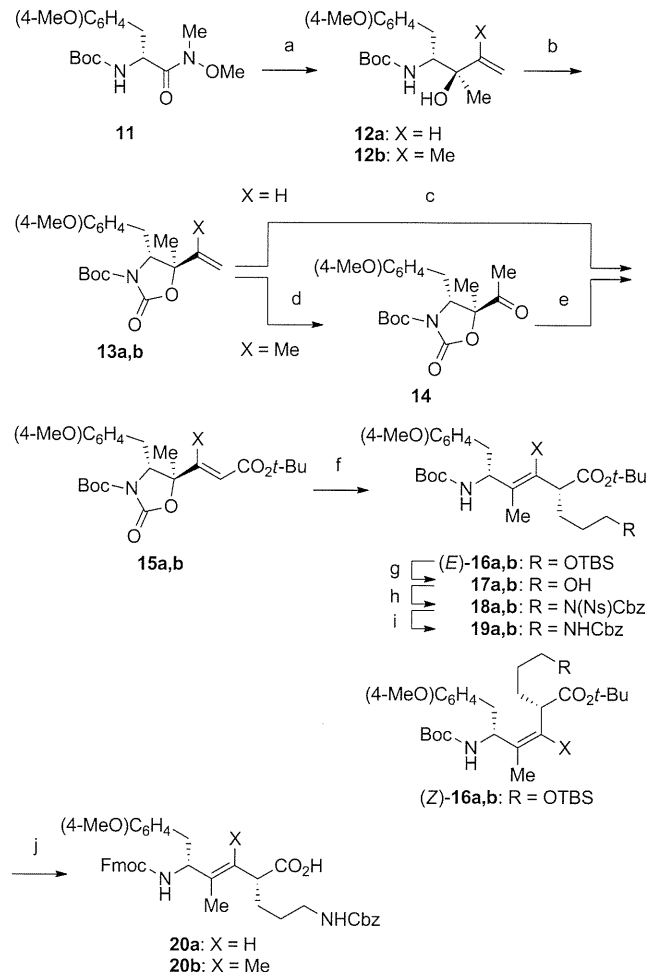


[a]Reagents and conditions: (a) (i) MeMgCl, THF, −78 °C, 1.5 h; (ii) $CH_2$=CXMgBr, $CeCl_3$, THF, 0 °C, 3 h; (iii) recrystallization (**12a**, 48%; **12b**, 47%); (b) NaH, THF, reflux, 1 h, then $(Boc)_2O$, rt, 2 h (**13a**, quantitative; **13b**, 87%); (c) (i) $O_3$, EtOAc, −78 °C, then $Me_2S$, −78 °C, 30 min; (ii) $(EtO)_2P(O)CH_2CO_2$-*t*-Bu, LiCl, $(i\text{-}Pr)_2NEt$, MeCN, 0 °C, 3.5 h (56%); (d) $O_3$, EtOAc, −78 °C, then $Me_2S$, −78 °C, 15 min (99%); (e) $Ph_3P$=$CHCO_2$-*t*-Bu, toluene, reflux, 10 h (quantitative); (f) TBSO$(CH_2)_3$Li, CuCN, LiCl, THF–$Et_2O$–*n*-pentane, −78 °C, 2 h (**16a**, 92%, *E*/*Z* = 80/20; **16b**, quantitative, *E*/*Z* = 79/21); (g) $H_2SiF_6$(aq), MeCN–$H_2O$, rt, 13.5 h (**17a**, 51%; **17b**, 91%); (h) NsNH(Cbz), DEAD, $PPh_3$, THF–toluene, 0 °C, overnight (**18a**, 61%; **18b**, quantitative); (i) PhSH, $K_2CO_3$, DMF, rt, overnight (**19a**, 81%; **19b**, 84%); (j) (i) TFA, $CH_2Cl_2$, rt, 2 h; (ii) FmocOSu, $(i\text{-}Pr)_2NEt$, MeCN–$H_2O$, rt, 14.5 h (**20a**, 57%; **20b**, 90%).

The epimeric D-Tyr-D-Orn dipeptide isostere **26** was also synthesized. Although a (*Z*)-selective HWE reaction[34] or modified Wittig reaction[35] of ketone **14** failed, Peterson olefination[36,37] provided an *E*/*Z* mixture of *α,β*-unsaturated esters in moderate yield (**15b**/**21** = 3/2) (Scheme 3). The mixture was converted to three *α*-alkylated products, namely, **22**, (*E*)-**16b**, and (*Z*)-**16b**. After cleavage of the TBS group, Mitsunobu reaction, and removal of the Ns group, a mixture of **25** and **19b** was separated from the (*Z*)-product derived from (*Z*)-**16b**. The desired D-Tyr-D-Orn isostere **26** was obtained via TFA-mediated deprotection and *N*-Fmoc protection, followed by separation from **20b** by column chromatography.

A representative synthesis of the isostere-containing FC131 derivatives is shown in Scheme 4. The protected peptide resin


dx.doi.org/10.1021/jm2016914 | J. Med. Chem. 2012, 55, 2746–2757

Scheme 3[a]

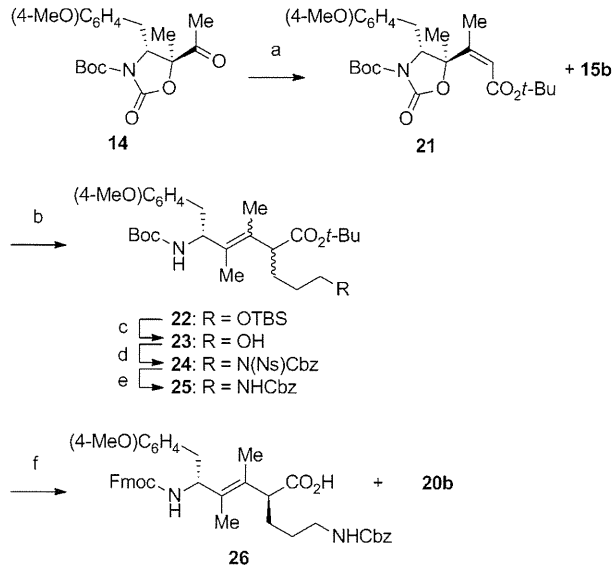


[a]Reagents and conditions: (a) $TMSCH_2CO_2$-*t*-Bu, LDA, THF–*n*-hexane, −78 °C, 4 h (53%, **15b**/**21** = 3/2); (b) $(TBS)O(CH_2)_3Li$, CuCN, LiCl, THF–$Et_2O$–*n*-pentane, −78 °C, 2 h (89%); (c) $H_2SiF_6$(aq), MeCN–$H_2O$, rt, 13.5 h (90%); (d) NsNH(Cbz), DEAD, $PPh_3$, THF–toluene, 0 °C, overnight (95%); (e) PhSH, $K_2CO_3$, DMF, rt, overnight (82%); (f) (i) TFA, $CH_2Cl_2$, rt, 2 h; (ii) FmocOSu, $(i\text{-}Pr)_2NEt$, MeCN–$H_2O$, rt, 14.5 h (**26**, 39%; **20b**, 54%).

Scheme 4[a]

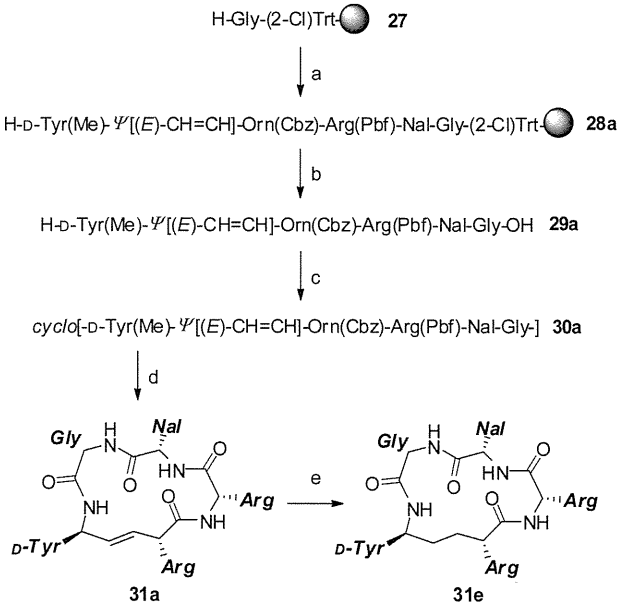


[a]Reagents and conditions: (a) Fmoc-based solid-phase peptide synthesis; (b) HFIP, $CH_2Cl_2$, rt, 2 h; (c) DPPA, $NaHCO_3$, DMF, −40 °C to rt, 48 h; (d) (i) TMSOTf–thioanisole in TFA, 0 °C to rt, 3.5 h; (ii) 1*H*-pyrazole-1-carboxamidine hydrochloride, $Et_3N$, DMF, rt, 2 days (22% from **27**); (e) $H_2$, Pd/$BaSO_4$, MeOH, rt, 36 h (33%).

**28a** was prepared on a 2-chlorotrityl [(2-Cl)Trt] resin using standard Fmoc-based solid-phase peptide synthesis. After cleavage of **28a** from the resin, the linear peptide **29a** was cyclized to **30a** using diphenylphosphoryl azide (DPPA). Removal of the side chain protecting groups in **30a** followed by conversion of the Orn $\delta$-amino group to a guanidino group using 1*H*-pyrazole-1-carboxamidine gave the expected peptide **31a** with a D-Tyr-Arg isostere. The derivatives **31b–d** were also obtained by the same procedure. In addition, an FC131 analogue, **31e**, with a D-Tyr-Arg ethylene isostere was prepared by hydrogenation of **31a** using Pd/$BaSO_4$.

**Structure–Activity Relationships of FC131 Derivatives for CXCR4 Binding.** We assessed the receptor binding of cyclic peptides **31a–e** with CXCR4 for inhibitory potency against [$^{125}$I]stromal-cell-derived factor-1 (SDF-1) binding to CXCR4 (Table 1). The biological activities of the disubstituted

**Table 1. Inhibitory Activity of FC131 Derivatives against SDF-1 Binding to CXCR4**

| peptide | sequence | $IC_{50}$[a] ($\mu$M) |
|---|---|---|
| FC131 | cyclo(-D-Tyr$^1$-L-Arg$^2$-L-Arg$^3$-L-Nal$^4$-Gly$^5$-) | 0.084 ± 0.037 |
| **31a** | cyclo(-D-Tyr$^1$-$\psi$[(*E*)-CH=CH]-L-Arg$^2$-L-Arg$^3$-L-Nal$^4$-Gly$^5$-) | 0.33 ± 0.074 |
| **31b** | cyclo(-D-Tyr$^1$-$\psi$[(*E*)-CMe=CH]-L-Arg$^2$-L-Arg$^3$-L-Nal$^4$-Gly$^5$-) | 0.50 ± 0.21 |
| **31c** | cyclo(-D-Tyr$^1$-$\psi$[(*E*)-CMe=CMe]-L-Arg$^2$-L-Arg$^3$-L-Nal$^4$-Gly$^5$-) | 2.5 ± 1.0 |
| **31d** | cyclo(-D-Tyr$^1$-$\psi$[(*E*)-CMe=CMe]-D-Arg$^2$-L-Arg$^3$-L-Nal$^4$-Gly$^5$-) | 0.10 ± 0.029 |
| **31e** | cyclo(-D-Tyr$^1$-$\psi$[$CH_2$–$CH_2$]-L-Arg$^2$-L-Arg$^3$-L-Nal$^4$-Gly$^5$-) | >10 |
| FC162 | cyclo(-D-Tyr$^1$-L-MeArg$^2$-L-Arg$^3$-L-Nal$^4$-Gly$^5$-) | 0.29 ± 0.12 |
| FC122 | cyclo(-D-Tyr$^1$-D-MeArg$^2$-L-Arg$^3$-L-Nal$^4$-Gly$^5$-) | 0.063 ± 0.032 |

[a]$IC_{50}$ values are the concentrations for 50% inhibition of the [$^{125}$I]SDF-1$\alpha$ binding to CXCR4 ($n$ = 3).

alkene-containing peptide **31a** and trisubstituted alkene-containing peptide **31b** were slightly less than that of FC131. These results suggested that the hydrogen-bonding capability of the D-Tyr$^1$–L-Arg$^2$ peptide bond in FC131 is not necessary, but is partly effective. The nearly equipotent activities of **31a** and **31b** indicated that the steric effects of a $\gamma$-methyl group of the alkene isostere in **31b**, which corresponds to the D-Tyr$^1$ carbonyl oxygen of FC131, are not critical to the antagonistic activity. Peptide **31c** containing a tetrasubstituted alkene isostere for D-Tyr$^1$-L-MeArg$^2$ exhibited low activity, whereas the D-MeArg$^2$ congener **31d** showed activity nearly equipotent to that of FC131. The bioactivity profile of the isostere-containing peptides was similar to that of a series of the parent peptides, including FC162 and FC122, except that their potencies were somewhat lower than those of the parents. These observations suggested that the *trans*-isomer of the D-Tyr$^1$–L/D-Arg$^2$ peptide bond contributes to the bioactivity of FC131 and its derivatives and that tri- and tetrasubstituted alkene isosteres closely mimic the D-Tyr$^1$-L-Arg$^2$ dipeptide and *N*-methylated congeners (D-Tyr$^1$-L-MeArg$^2$ and D-Tyr$^1$-D-MeArg$^2$), respectively. On the other hand, an ethylene isostere-containing analogue, **31e**, did not bind with CXCR4. The increased flexibility of the peptide backbone as a result of the ethylene substructure led to a higher entropy loss upon receptor binding, indicating that the fixed planar structure of the D-Tyr$^1$–L-Arg$^2$ peptide bond is indispensable for biological activity.

**Molecular Modeling Study of Cyclic Peptidomimetics and Identification of an Alternative Binding Mode of Cyclic Pentapeptide CXCR4 Antagonists.** To investigate the bioactive conformations of cyclic pentapeptide-based CXCR4 antagonists, the $^1$H NMR spectra of **31a–d** were obtained. Peptides **31a–c** showed nuclear Overhauser effect


dx.doi.org/10.1021/jm2016914 | J. Med. Chem. 2012, 55, 2746–2757

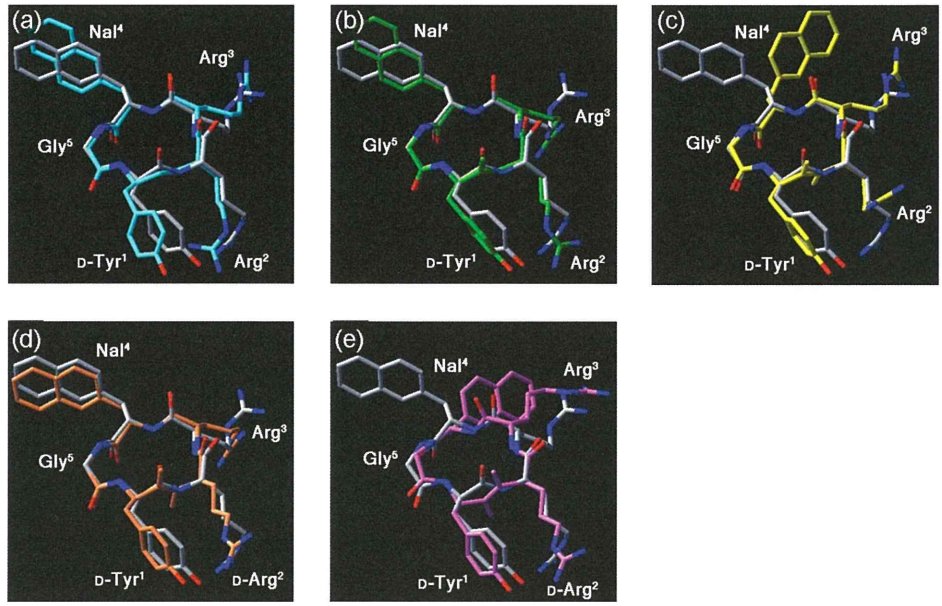


**Figure 4.** Superimposed low-energy structures of FC131 (gray) and the isostere-containing derivatives: (a) **31a** (blue), (b) **31b** (green), (c) **31c** (yellow), (d) **31d-A** (orange), and (e) **31d-B** (pink).

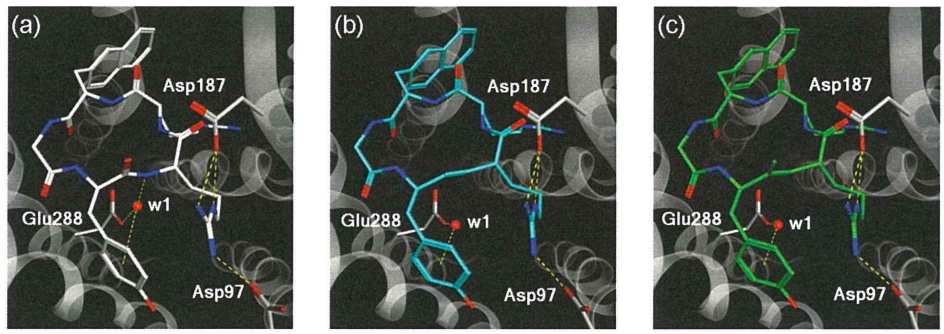


**Figure 5.** Binding modes of FC131 derivatives: (a) FC131, (b) **31a**, and (c) **31b**.

(NOE) patterns around the isostere similar to those seen with FC131. Interestingly, the D-Tyr$^1$-D-MeArg$^2$ isostere-containing **31d** existed as a 1:1 mixture of two conformers; one conformer, **31d-A**, exhibited NOE patterns similar to those of FC131, and the other conformer, **31d-B**, showed different patterns. We also calculated their low-energy conformations in solution using a molecular dynamics simulation based on the NMR data. The calculations were performed by MacroModel using the Merck molecular force field (MMFFs). The backbone conformations of peptides **31a–c** and **31d-A** were similar to that of FC131 (Figure 4a–d), but **31d-B** exhibited a conformation different from that of FC131 with respect to the orientation around the isostere alkene substructure in the D-Tyr$^1$-D-MeArg$^2$ dipeptide (Figure 4e).

Recently, we and others have reported pharmacophore models and binding models of FC131.[38−41] In our FC131–CXCR4 complex model,[41] using NMR-based calculated conformations of FC131[20,22] and an X-ray crystal structure of CXCR4[42] (Figure 5a), a guanidino group of L-Arg$^2$ interacts with both Asp97 and Asp187 in CXCR4, and an amide proton of L-Arg$^2$ forms a hydrogen bond network with Glu288 via a crystal water molecule (**w1**), which is also involved in an OH–$\pi$ interaction with an aromatic ring of D-Tyr$^1$. The L-Arg$^3$ guanidino group interacts with His113, Thr117, and Asp171 in CXCR4. In addition, the carbonyl oxygen of L-Nal$^4$ is involved in a second hydrogen bond network including Tyr255 and Glu288 side chains via another crystal water molecule, and hydrogen bonds are present between D-Tyr$^1$ phenol and Tyr45 phenol and between the carbonyl oxygen of Gly$^5$ and the Ser285 hydroxyl group (see the Supporting Information). Most of these interactions were maintained in all the following binding conformations of FC131 derivatives.

Using this FC131–CXCR4 complex model, we next carried out a prediction of the binding mode for **31a–d** with CXCR4. Models for binding of **31a–d** with CXCR4 were obtained by energy minimization of the complex structure using the MMFF94s force field in the Molecular Operating Environment (MOE) software package[43] (Figures 5–7). The global conformation of FC131 was little altered by substitution of the D-Tyr$^1$-L-Arg$^2$ substructure with a disubstituted [$\psi$[(*E*)-CH=CH]] alkene unit in **31a** (Figure 5b). The interactions of the L-Arg$^2$ guanidino group and the OH–$\pi$ interaction of the D-Tyr$^1$ phenol group with the water molecule (**w1**) were also maintained. The slightly less potent binding of **31a** may be attributable to the loss of the hydrogen bond networks by the D-Tyr$^1$–L-Arg$^2$ peptide bond. Peptide **31b** with a $\psi$[(*E*)-CMe=CH] isosteric unit also exhibited a binding conformation similar to that of FC131 with the same interaction modes as those of **31a** with CXCR4 (Figure 5c). The similar biological activities and binding modes of **31a** and **31b** suggested that the


dx.doi.org/10.1021/jm2016914 | *J. Med. Chem.* 2012, 55, 2746–2757

steric effect of the D-Tyr[1] carbonyl oxygen in FC131 and the γ-methyl group of the isostere unit in **31b** did not cause any favorable or unfavorable interactions with CXCR4. This may be a result of the outward orientation of the D-Tyr[1] carbonyl group in FC131 from the receptor.

The whole backbone conformation of **31c** was also maintained (Figure 6b), whereas the water molecule (**w1**) was not settled below the antagonist because of the isostere β-methyl group. The lower potency of **31c** than that of **31a,b** could be rationalized by the loss of the **w1**-mediated OH−π interaction. Similarly, it was suggested that the lower receptor binding of the parent FC162 compared with that of FC131 was a result of the *N*-methyl group of L-MeArg[2] in FC162 preventing the OH−π interaction (Figure 6a).

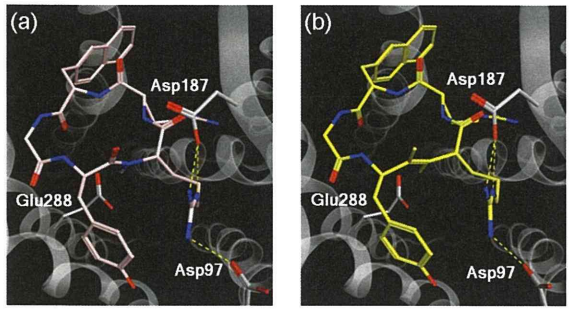


**Figure 6.** Binding modes of FC131 derivatives: (a) FC162 and (b) **31c**.

A calculation using the FC131-like conformer **31d-A** as an initial structure afforded a binding mode for **31d** similar to that of **31a−c**; however, the binding mode failed to provide a possible explanation for the improved bioactivity of **31d**. In contrast, an alternative reasonable binding mode of **31d** with CXCR4 was obtained when another conformation, **31d-B**, with the flipped alkene substructure was used for the calculation (Figure 7b). In this model, peptide **31d** was bound to CXCR4 at a slightly different position on CXCR4 with the **w1**-mediated OH−π interaction maintained, and the D-MeArg[2] guanidino group of **31d** bound only with Asp187 via bimodal interactions. The isostere β-methyl group may possibly restrict the peptide backbone structure to a low-energy conformation such as **31d-B**, observed in NMR analysis, which leads to decreased entropy loss upon receptor binding.

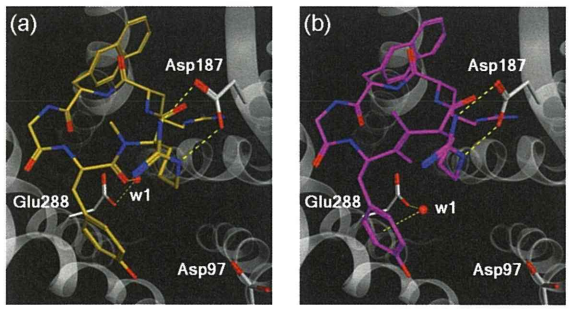


**Figure 7.** Binding modes of FC131 derivatives: (a) FC122 and (b) **31d**.

The binding-mode analysis of the most potent FC122 using NMR-based conformations afforded a binding structure similar to that of FC131 (data not shown); however, the highly potent activity of FC122 could not be fully rationalized by this binding mode. A possible alternative binding mode of FC122 was obtained on the basis of the characteristic binding mode of **31d**, which is the isosteric peptide corresponding to FC122 with a D-Tyr[1]-D-MeArg[2] substructure (Figure 7a). Although the binding structure of FC122 was inconsistent with its NMR-based structure with respect to the orientation of the D-Tyr[1]−D-MeArg[2] peptide bond,[41] the local conformation and binding mode around the D-Tyr[1]−D-MeArg[2] peptide bond in FC122 were similar to those of **31d**. In this binding mode, the *N*-methyl group of D-MeArg[2] in FC122 probably restricts the peptide backbone conformation, as does the isostere β-methyl group in **31d**. The less potent bioactivity of **31d** compared with that of the isosteric FC122 accounted for these similar binding modes. The D-Tyr[1] carbonyl oxygen in FC122 formed a hydrogen bond network via a water molecule (**w1**), but in **31d**, the corresponding hydrogen bond was missing because of the isosteric tetrasubstituted alkene.

In this study, docking simulations of FC131 derivatives were performed using the X-ray crystal structure of CXCR4 in a complex with a 16-residue cyclic peptide, CVX15.[42] The binding modes of FC131 and its derivatives met the requirements of the shared indispensable functional groups between CVX15 and FC131: the L-Arg[3] guanidino group and L-Nal[4] naphthalene group in FC131 correspond to Arg[2] and Nal[3] in CVX15, respectively. Although the backbone conformations varied in the cases of FC122 and **31d** as a result of the substitution mode of the D-Tyr[1]−D-MeArg[2] peptide bond, the binding modes of the side chain functional groups were maintained.

## CONCLUSIONS

To investigate bioactive conformations, four alkene isosteres for D-Tyr[1]-L/D-Arg[2] dipeptides in the selective CXCR4 antagonist FC131 and its derivatives were synthesized. The bioactivity profiles of a series of the cyclic peptidomimetics suggested that the D-Tyr[1]−L-Arg[2] and D-Tyr[1]−L/D-MeArg[2] peptide bonds of the FC131 derivatives existed as *trans*-conformers in the bioactive conformations. In the SAR study, the tetrasubstituted alkene dipeptide isosteres adequately mimicked the *N*-methylamide bonds in D-Tyr[1]-L-MeArg[2] and D-Tyr[1]-D-MeArg[2] dipeptides. NMR studies indicated that the backbone structures of all the isostere-containing derivatives in solution were similar to that of FC131, except that a different orientation of the isostere alkene substructure was observed in **31d-B**, containing a D-Tyr[1]-D-MeArg[2] isostere. A comparative biological evaluation and binding-mode prediction suggest that the L-Arg[2] amide hydrogen in FC131 is involved in indirect receptor binding via water molecules. Although the addition of a methyl group on the D-Tyr[1]−L-Arg[2] peptide bond (FC162) or the corresponding isostere β-position (**31c**) did not influence the peptide conformation in a complex with CXCR4, the potential hydrogen bond network via water molecules in FC131 was eliminated. On the other hand, an alternative binding mode was identified in the D-MeArg[2] congener **31d**, which is the best among the isostere-containing peptides. On the basis of this binding mode of **31d**, the previously unknown binding mode of the D-MeArg[2]-substituted peptide (FC122) was identified; this was not calculated directly from the NMR-based conformations. On the basis of this binding mode for CXCR4, it is concluded that the improved potency of FC122 may be derived from a secondary conformation stabilized by both chirality and the *N*-methyl group of D-MeArg[2]. These results suggest that two distinct binding modes of cyclic pentapeptide-based


dx.doi.org/10.1021/jm2016914 | J. Med. Chem. 2012, 55, 2746−2757

CXCR4 antagonists may provide new insights into the design of more potent derivatives and small-molecule antagonists with novel scaffolds.

## EXPERIMENTAL SECTION

**General Procedures.** All moisture-sensitive reactions were performed using syringe−septum cap techniques under an argon atmosphere, and all glassware was dried in an oven at 80 °C for 2 h prior to use. Melting points were measured by a hot stage melting point apparatus and are uncorrected. Optical rotations were measured with a JASCO P-1020 polarimeter. For flash chromatography, Wakogel C-300E was employed. For analytical HPLC, a COSMOSIL 5C18-ARII column (4.6 × 250 mm, Nacalai Tesque Inc., Kyoto, Japan) was employed with a linear gradient of MeCN containing 0.1% (v/v) TFA at a flow rate of 1 mL/min on a Shimadzu LC-20ADvp (Shimadzu Corp., Ltd., Kyoto, Japan). Preparative HPLC was performed using a COSMOSIL 5C18-ARII column (20 × 250 mm, Nacalai Tesque Inc.) with a linear gradient of MeCN containing 0.1% (v/v) TFA at a flow rate of 8 mL/min on a Shimadzu LC-6AD (Shimadzu Corp., Ltd.). $^1$H NMR spectra were recorded using a JEOL ECA-500 spectrometer, and chemical shifts are reported in $\delta$ (ppm) relative to TMS (in $CDCl_3$) or DMSO (in DMSO-$d_6$) as an internal standard. $^{13}$C NMR spectra were recorded using a JEOL ECA-500 spectrometer and referenced to the residual $CHCl_3$ or DMSO signal. Chemical shifts were reported in parts per million with the residual solvent peak used as an internal standard. $^1$H NMR spectral data are given as follows: chemical shift, multiplicity (br = broad, s = singlet, d = doublet, t = triplet, q = quartet, m = multiplet), number of protons, and coupling constant(s). Exact mass (HRMS) spectra were recorded on a JMS-HX/HX 110A mass spectrometer. Infrared (IR) spectra were obtained on a JASCO FT/IR-4100 FT-IR spectrometer with a JASCO ATR PRO410-S. The purity of the peptides for bioassay was calculated as >95% by HPLC on a COSMOSIL 5C18-ARII analytical column at 220 nm absorbance (see the Supporting Information).

**(3*R*,4*R*)-4-[*N*-(*tert*-Butoxycarbonyl)amino]-5-(4-methoxyphenyl)pent-1-en-3-ol (2).** To a solution of LiCl (4.11 g, 96.9 mmol) and $ZnCl_2$ (13.2 g, 96.9 mmol) in THF (50 mL) was added dropwise a solution of vinylmagnesium bromide in THF (1.3 M, 75.0 mL, 96.9 mmol) at −78 °C under argon, and the mixture was stirred at 0 °C for 30 min. To a solution of Boc-L-Tyr(Me)OMe (10.0 g, 32.3 mmol) in $CH_2Cl_2$ (40 mL) and toluene (80 mL) was added dropwise a solution of DIBAL-H in toluene (0.99 M, 72.0 mL, 71.1 mmol) at −78 °C under argon, and the mixture was stirred at −78 °C for 30 min. To this solution was added dropwise the above solution of vinylzinc reagent at −78 °C, and the mixture was stirred for 3 h with warming to 0 °C. The reaction was quenched with 0.5 M Rochelle salt and saturated $NH_4Cl$. The mixture was concentrated under reduced pressure and extracted with EtOAc. The extract was washed with saturated citric acid, brine, saturated $NaHCO_3$, and brine and dried over $MgSO_4$. Concentration under reduced pressure followed by flash chromatography over silica gel with *n*-hexane−EtOAc (4:1) gave the title compound **2** (3.07 g, 9.99 mmol, 31% yield) as white solids: mp 91−92 °C; $[\alpha]_D^{28}$ +27.9 (*c* 1.39, $CHCl_3$); IR (neat) 3323 (OH and NH), 1696 (C=O); $^1$H NMR (500 MHz, $CDCl_3$) $\delta$ 1.39 (s, 9H), 2.29−2.39 (m, 1H), 2.75−2.85 (m, 1H), 2.88 (dd, *J* = 13.7, 7.4 Hz, 1H), 3.69−3.77 (m, 1H), 3.78 (s, 3H), 4.07−4.14 (m, 1H), 4.79 (d, *J* = 6.3 Hz, 1H), 5.18 (d, *J* = 10.3 Hz, 1H), 5.27 (d, *J* = 17.2 Hz, 1H), 5.89 (ddd, *J* = 17.2, 10.3, 5.7 Hz, 1H), 6.83 (d, *J* = 8.6 Hz, 2H), 7.15 (d, *J* = 8.6 Hz, 2H); $^{13}$C NMR (125 MHz, $CDCl_3$) $\delta$ 28.3 (3C), 37.0, 55.2, 56.1, 72.6, 79.4, 113.9 (2C), 116.0, 130.3 (3C), 138.4, 156.2, 158.2; HRMS (FAB) *m*/*z* calcd for $C_{17}H_{26}NO_4$ ($MH^+$) 308.1856, found 308.1855.

**(3*R*,4*R*)-4-[*N*-(*tert*-Butoxycarbonyl)amino]-5-(4-methoxyphenyl)pent-1-en-3-yl Acetate (3).** To a solution of the alcohol **2** (368.9 mg, 1.20 mmol) in $CHCl_3$ (12 mL) were added pyridine (1.94 mL, 24.0 mmol), $Ac_2O$ (1.13 mL, 12.0 mmol), and 4-(dimethylamino)pyridine (DMAP; 14.7 mg, 0.12 mmol) at 0 °C, and the mixture was stirred for 2 h at the same temperature. The reaction was quenched with saturated $NH_4Cl$ at 0 °C. The mixture was concentrated under reduced pressure and extracted with EtOAc. The extract was washed successively with 1 N HCl, brine, 5% $NaHCO_3$, and brine and dried over $MgSO_4$. Concentration under reduced pressure followed by flash chromatography over silica gel with *n*-hexane−EtOAc (4:1) gave the title compound **3** (418 mg, 1.20 mmol, quantitative) as colorless crystals: mp 96−97 °C; $[\alpha]_D^{26}$ +48.8 (*c* 1.21, $CHCl_3$); IR (neat) 3355 (NH), 1742 (C=O), 1712 (C=O); $^1$H NMR (500 MHz, $CDCl_3$) $\delta$ 1.39 (s, 9H), 2.12 (s, 3H), 2.72 (d, *J* = 6.9 Hz, 2H), 3.78 (s, 3H), 3.96−4.07 (m, 1H), 4.67 (d, *J* = 9.2 Hz, 1H), 5.18−5.30 (m, 3H), 5.74−5.84 (m, 1H), 6.82 (d, *J* = 8.6 Hz, 2H), 7.08 (d, *J* = 8.6 Hz, 2H); $^{13}$C NMR (125 MHz, $CDCl_3$) $\delta$ 21.0, 28.3 (3C), 37.5, 54.3, 55.2, 74.4, 79.4, 113.9 (2C), 118.0, 129.3, 130.2 (2C), 133.7, 155.4, 158.3, 169.7; HRMS (FAB) *m*/*z* calcd for $C_{19}H_{28}NO_5$ ($MH^+$) 350.1962, found 350.1958.

***tert*-Butyl (4*R*,5*R*,2*E*)-4-Acetoxy-5-[*N*-(*tert*-butoxycarbonyl)-amino]-6-(4-methoxyphenyl)hex-2-enoate (4).** Ozone gas was bubbled through a stirred solution of the acetate **3** (3.29 g, 9.50 mmol) in EtOAc (95 mL) at −78 °C until a blue color persisted. $Me_2S$ (14.0 mL, 190 mmol) was added to the solution at −78 °C. After being stirred for 30 min at 0 °C, the mixture was dried over $MgSO_4$ and concentrated under reduced pressure to give the crude aldehyde, which was used for the next reaction without further purification. To a stirred suspension of LiCl (805 mg, 19.0 mmol) in MeCN (35 mL) was added *tert*-butyl diethylphosphonoacetate (4.79 g, 19.0 mmol) in MeCN (30 mL) and $(i\text{-Pr})_2$NEt (3.31 mL, 19.0 mmol) at 0 °C under argon. After 20 min, the above aldehyde in MeCN (30 mL) was added to the mixture at 0 °C, and the stirring was continued for 3 h. The reaction was quenched with saturated $NH_4Cl$ at 0 °C. The mixture was concentrated under reduced pressure and extracted with EtOAc. The extract was washed successively with saturated citric acid, brine, 5% $NaHCO_3$, and brine and dried over $MgSO_4$. Concentration under reduced pressure followed by flash chromatography over silica gel with *n*-hexane−EtOAc (4:1) gave the title compound **4** (2.63 g, 5.85 mmol, 62% yield) as a colorless oil: $[\alpha]_D^{23}$ +44.7 (*c* 1.24, $CHCl_3$); IR (neat) 1706 (C=O); $^1$H NMR (500 MHz, $CDCl_3$) $\delta$ 1.39 (s, 9H), 1.45 (s, 9H), 2.13 (s, 3H), 2.72 (d, *J* = 6.9 Hz, 2H), 3.77 (s, 3H), 3.97−4.15 (m, 1H), 4.50−4.70 (m, 1H), 5.38 (ddd, *J* = 5.2, 2.9, 1.1 Hz, 1H), 5.81 (dd, *J* = 15.5, 1.1 Hz, 1H), 6.69 (dd, *J* = 15.5, 5.2 Hz, 1H), 6.82 (d, *J* = 8.6 Hz, 2H), 7.06 (d, *J* = 8.6 Hz, 2H); $^{13}$C NMR (125 MHz, $CDCl_3$) $\delta$ 20.3, 27.6 (3C), 27.9 (3C), 36.9, 53.7, 54.7, 72.4, 79.0, 80.1, 113.6 (2C), 124.2, 128.7, 129.7 (2C), 141.4, 154.9, 158.1, 164.4, 169.0; HRMS (FAB) *m*/*z* calcd for $C_{24}H_{34}NO_7$ ($MH^-$) 448.2341, found 448.2344.

***tert*-Butyl (4*R*,5*R*,2*E*)-5-[*N*-(*tert*-Butoxycarbonyl)amino]-4-hydroxy-6-(4-methoxyphenyl)hex-2-enoate (5).** To a solution of the acetate **4** (1.21 g, 2.70 mmol) in MeOH (27 mL) was added $K_2CO_3$ (746 mg, 5.40 mmol) at 0 °C, and the mixture was stirred for 2 h at room temperature. After the mixture was filtered, the filtrate was concentrated under reduced pressure and extracted with EtOAc. The extract was washed with brine and dried over $MgSO_4$. Concentration under reduced pressure followed by flash chromatography over silica gel with *n*-hexane−EtOAc (3:1) gave the title compound **5** (1.06 g, 2.60 mmol, 96% yield) as colorless solids: mp 98−99 °C; $[\alpha]_D^{24}$ +60.3 (*c* 1.04, $CHCl_3$); IR (neat) 3436 (OH and NH), 1698 (C=O); $^1$H NMR (500 MHz, $CDCl_3$) $\delta$ 1.38 (s, 9H), 1.45 (s, 9H), 2.81 (dd, *J* = 13.7, 7.4 Hz, 1H), 2.90 (dd, *J* = 13.7, 7.4 Hz, 1H), 3.75 (s, 3H), 3.77−3.85 (m, 1H), 4.23−4.27 (m, 1H), 4.96−5.05 (m, 1H), 5.98 (dd, *J* = 15.5, 1.7 Hz, 1H), 6.78−6.84 (m, 3H), 7.14 (d, *J* = 8.6 Hz, 2H); $^{13}$C NMR (125 MHz, $CDCl_3$) $\delta$ 28.0 (3C), 28.2 (3C), 36.8, 55.06, 55.09, 70.8, 79.5, 80.3, 114.0 (2C), 123.3, 130.07 (2C), 130.10, 146.8, 156.0, 158.3, 165.6. Anal. Calcd for $C_{22}H_{33}NO_6$: C, 64.84; H, 8.16; N, 3.44. Found: C, 64.67; H, 8.19; N, 3.55.

***tert*-Butyl (4*R*,5*R*,2*E*)-5-[*N*-(*tert*-Butoxycarbonyl)amino]-4-[(methylsulfonyl)oxy]-6-(4-methoxyphenyl)hex-2-enoate (6).** To a stirred solution of the alcohol **5** (897 mg, 2.20 mmol) in $CH_2Cl_2$ (22 mL) were added $Et_3N$ (3.06 mL, 22.0 mmol) and methanesulfonyl chloride (851 μL, 11.0 mmol) at 0 °C, and the mixture was stirred for 2 h at the same temperature. After the reaction was quenched with water, the mixture was concentrated under reduced pressure, and the residue was extracted with EtOAc. The extract was

washed with brine and dried over $MgSO_4$. Concentration under reduced pressure followed by recrystallization from *n*-hexane−EtOAc (10:1) gave the title compound **6** (1.03 g, 2.12 mmol, 96% yield) as colorless crystals: mp 145−146 °C; $[\alpha]_D^{22}$ +42.3 (*c* 1.00, $CHCl_3$); IR (neat) 3372 (NH), 1707 (C=O); $^1$H NMR (500 MHz, $CDCl_3$) $\delta$ 1.38 (s, 9H), 1.47 (s, 9H), 2.74 (dd, *J* = 14.3, 8.0 Hz, 1H), 2.89 (dd, *J* = 14.3, 6.9 Hz, 1H), 3.06 (s, 3H), 3.78 (s, 3H), 4.04−4.13 (m, 1H), 4.71 (d, *J* = 9.2 Hz, 1H), 5.18−5.24 (m, 1H), 6.02 (d, *J* = 15.5 Hz, 1H), 6.78 (dd, *J* = 15.5, 5.7 Hz, 1H), 6.84 (d, *J* = 8.6 Hz, 2H), 7.16 (d, *J* = 8.6 Hz, 2H); $^{13}$C NMR (125 MHz, $CDCl_3$) $\delta$ 28.0 (3C), 28.2 (3C), 36.6, 39.2, 54.9, 55.2, 80.0, 80.3, 81.2, 114.0 (2C), 126.9, 128.5, 130.2 (2C), 139.2, 155.1, 158.5, 164.3. Anal. Calcd for $C_{23}H_{35}NO_8S$: C, 56.89; H, 7.26; N, 2.88. Found: C, 56.96; H, 7.03; N, 2.85.

***tert*-Butyl (2*R*,5*R*,3*E*)-5-[*N*-(*tert*-Butoxycarbonyl)amino]-2-[3-(*tert*-butyldimethylsiloxy)propyl]-6-(4-methoxyphenyl)hex-3-enoate (7).** To a suspension of CuCN (1.79 g, 20.0 mmol) and LiCl (1.70 g, 40.0 mmol) in THF (40 mL) was added dropwise a solution of $TBSO(CH_2)_3Li$ in *n*-pentane−$Et_2O$ (0.5 M, 40.0 mL, 20.0 mmol) at −78 °C under argon, and the mixture was stirred for 30 min at 0 °C. To the above mixture was added dropwise a solution of the mesylate **6** (2.43 g, 5.0 mmol) in THF (20 mL) at −78 °C, and the mixture was stirred for 30 min at −78 °C. The reaction was quenched at −78 °C by the addition of a saturated $NH_4Cl$/28% $NH_4OH$ solution (1:1, 50 mL), with additional stirring at room temperature for 3 h. After the mixture was concentrated under reduced pressure, the residue was extracted with $Et_2O$. The extract was washed with water and brine and dried over $MgSO_4$. Concentration under reduced pressure followed by flash chromatography over silica gel with *n*-hexane−EtOAc (6:1) gave the title compound **7** (2.64 g, 4.68 mmol, 94% yield) as a colorless oil: $[\alpha]_D^{23}$ −14.9 (*c* 1.09, $CHCl_3$); IR (neat) 3372 (NH), 1715 (C=O); $^1$H NMR (500 MHz, $CDCl_3$) $\delta$ 0.04 (s, 6H), 0.89 (s, 9H), 1.28−1.48 (m, 21H), 1.66−1.75 (m, 1H), 2.62−2.87 (m, 3H), 3.56 (t, *J* = 6.3 Hz, 2H), 3.77 (s, 3H), 4.25−4.51 (m, 2H), 5.40−5.52 (m, 2H), 6.81 (d, *J* = 8.0 Hz, 2H), 7.09 (d, *J* = 8.0 Hz, 2H); $^{13}$C NMR (125 MHz, $CDCl_3$) $\delta$ −5.4 (2C), 18.3, 25.9 (3C), 28.0 (3C), 28.3 (3C), 28.9, 30.0, 40.8, 49.5, 52.8, 55.1, 62.6, 79.2, 80.4, 113.7 (2C), 128.9, 129.4, 130.5 (2C), 132.1, 155.0, 158.2, 173.3; HRMS (FAB) *m*/*z* calcd for $C_{31}H_{54}NO_6Si$ ($MH^+$) 564.3715, found 564.3712.

***tert*-Butyl (2*R*,5*R*,3*E*)-2-{3-[*N*-[(Benzyloxy)carbonyl]-*N*-[(2-nitrophenyl)sulfonyl]amino]propyl}-5-[*N*-(*tert*-butoxycarbonyl)amino]-6-(4-methoxyphenyl)hex-3-enoate (8).** To a solution of the TBS ether **7** (2.59 g, 4.60 mmol) in MeCN−$H_2O$ (1:1, 46 mL) was added aqueous $H_2SiF_6$ (3.28 M, 701 $\mu$L, 2.30 mmol) at 0 °C, and the mixture was stirred at room temperature for 2 h. After the mixture was concentrated, the residue was extracted with EtOAc. The extract was washed with 5% $K_2CO_3$ and brine and dried over $MgSO_4$. Concentration under reduced pressure gave the corresponding alcohol, which was used in the next step without further purification. To a solution of the alcohol, $PPh_3$ (1.81 g, 6.90 mmol), and NsNH(Cbz) (1.70 g, 5.06 mmol) in THF (50 mL) was added diethyl azodicarboxylate (DEAD) in toluene (2.2 M, 2.51 mL, 5.52 mmol) at 0 °C under argon, and the mixture was stirred at the same temperature for 3 h. The reaction was quenched at 0 °C by the addition of MeOH (10 mL), with additional stirring at the same temperature for 30 min. Concentration under reduced pressure followed by flash chromatography over silica gel with *n*-hexane−EtOAc (3:1) gave the title compound **8** (3.03 g, 3.95 mmol, 86% yield) as a colorless oil: $[\alpha]_D^{22}$ −11.0 (*c* 1.10, $CHCl_3$); IR (neat) 3411 (NH), 1720 (C=O); $^1$H NMR (500 MHz, $CDCl_3$) $\delta$ 1.41 (s, 9H), 1.42 (s, 9H), 1.46−1.56 (m, 1H), 1.65−1.78 (m, 3H), 2.70−2.83 (m, 2H), 2.84−2.91 (m, 1H), 3.76 (s, 3H), 3.83 (t, *J* = 7.4 Hz, 2H), 4.21−4.61 (m, 2H), 5.10 (s, 2H), 5.43−5.53 (m, 2H), 6.82 (d, *J* = 8.6 Hz, 2H), 7.08 (d, *J* = 8.6 Hz, 2H), 7.18−7.23 (m, 2H), 7.29−7.36 (m, 3H), 7.41−7.47 (m, 1H), 7.62−7.71 (m, 2H), 8.09 (d, *J* = 8.0 Hz, 1H); $^{13}$C NMR (125 MHz, $CDCl_3$) $\delta$ 27.4, 27.9 (3C), 28.3 (3C), 29.2, 40.6, 47.7, 49.2, 52.8, 55.1, 69.3, 79.1, 80.6, 113.6 (2C), 124.2, 128.4 (2C), 128.6 (2C), 128.7, 129.3, 130.0, 130.4, 130.5, 131.5, 132.4, 132.7, 134.0 (2C), 134.2, 147.6, 151.6, 155.0, 158.1, 172.8; HRMS (FAB) *m*/*z* calcd for $C_{39}H_{48}N_3O_{11}S$ ($MH^-$) 766.3015, found 766.3011.

***tert*-Butyl (2*R*,5*R*,3*E*)-2-{3-[*N*-[(Benzyloxy)carbonyl]amino]-propyl}-5-[*N*-(*tert*-butoxycarbonyl)amino]-6-(4-methoxyphenyl)hex-3-enoate (9).** To a stirred solution of enoate **8** (2.69 g, 3.50 mmol) in DMF (35 mL) were added thiophenol (715 $\mu$L, 7.00 mmol) and $K_2CO_3$ (1.45 g, 10.5 mmol) at room temperature, and the mixture was stirred at the same temperature for 3 h. After concentration under reduced pressure, the residue was extracted with EtOAc, washed with saturated citric acid, brine, 5% $NaHCO_3$, and brine, and dried over $MgSO_4$. Concentration under reduced pressure followed by flash chromatography over silica gel with *n*-hexane−EtOAc (3:1) gave the title compound **9** (1.95 g, 3.35 mmol, 96% yield) as a colorless oil: $[\alpha]_D^{22}$ −19.8 (*c* 1.09, $CHCl_3$); IR (neat) 3342 (NH), 1700 (C=O); $^1$H NMR (500 MHz, $CDCl_3$) $\delta$ 1.31−1.43 (m, 21H), 1.60−1.68 (m, 1H), 2.64−2.72 (m, 1H), 2.76−2.85 (m, 2H), 3.06−3.17 (m, 2H), 3.75 (s, 3H), 4.27−4.37 (m, 1H), 4.50−4.60 (m, 1H), 4.83−4.91 (m, 1H), 5.09 (s, 2H), 5.39−5.48 (m, 2H), 6.80 (d, *J* = 8.0 Hz, 2H), 7.06 (d, *J* = 8.0 Hz, 2H), 7.27−7.37 (m, 5H); $^{13}$C NMR (125 MHz, $CDCl_3$) $\delta$ 27.2, 27.9 (3C), 28.3 (3C), 29.4, 40.6 (2C), 49.3, 52.9, 55.1, 66.5, 79.2, 80.6, 113.6 (2C), 127.96 (2C), 128.01, 128.4 (2C), 128.7, 129.4, 130.4 (2C), 132.4, 136.5, 155.0, 156.3, 158.1, 173.0; HRMS (FAB) *m*/*z* calcd for $C_{33}H_{45}N_2O_7$ ($MH^-$) 581.3232, found 581.3239.

**(2*R*,5*R*,3*E*)-2-{3-[*N*-[(Benzyloxy)carbonyl]amino]propyl}-5-{*N*-[(9-fluorenylmethoxy)carbonyl]amino}-6-(4-methoxyphenyl)-hex-3-enoic Acid (10).** To a stirred solution of enoate **9** (1.11 g, 1.90 mmol) in $CH_2Cl_2$ (20 mL) was added trifluoroacetic acid (5 mL), and the mixture was stirred for 2 h at room temperature. After concentration under reduced pressure, the residue was dissolved in water (10 mL). To this solution were added $Et_3N$ (792 $\mu$L, 5.70 mmol) and FmocOSu (641 mg, 1.90 mmol) in MeCN (10 mL) at 0 °C, and the mixture was stirred for 2 h at room temperature. The reaction was quenched by addition of 1 N HCl. After concentration under reduced pressure, the residue was extracted with EtOAc. The extract was washed with 1 N HCl and brine and dried over $MgSO_4$. Concentration under reduced pressure followed by flash chromatography over silica gel with *n*-hexane−EtOAc (1:1) containing 1% AcOH gave the title compound **10** (875 mg, 1.35 mmol, 71% yield) as colorless solids: mp 166−167 °C; $[\alpha]_D^{22}$ +1.7 (*c* 1.09, DMSO); IR (neat) 1705 (C=O); $^1$H NMR (500 MHz, DMSO-$d_6$) $\delta$ 1.26−1.46 (m, 3H), 1.52−1.69 (m, 1H), 2.70 (d, *J* = 6.9 Hz, 2H), 2.85−2.93 (m, 1H), 2.94−3.04 (m, 2H), 3.67 (s, 3H), 4.12−4.27 (m, 4H), 5.03 (s, 2H), 5.46 (dd, *J* = 15.5, 8.6 Hz, 1H), 5.57 (dd, *J* = 15.5, 5.7 Hz, 1H), 6.80 (d, *J* = 8.0 Hz, 2H), 7.13 (d, *J* = 8.0 Hz, 2H), 7.25−7.39 (m, 8H), 7.39−7.45 (m, 2H), 7.51 (d, *J* = 8.6 Hz, 1H), 7.63−7.71 (m, 2H), 7.88 (d, *J* = 7.4 Hz, 2H), 12.3 (s, 1H); $^{13}$C NMR (125 MHz, DMSO-$d_6$) $\delta$ 27.0, 29.3, 40.0 (2C, overlapped with DMSO peaks), 46.7, 48.0, 54.2, 54.9, 65.2, 65.3, 113.5 (2C), 120.1 (2C), 125.3 (2C), 127.1 (2C), 127.6 (2C), 127.7 (2C), 127.7, 128.1, 128.4 (2C), 130.3 (2C), 130.4, 133.0 (2C), 137.3, 140.7 (2C), 143.9 (2C), 155.4, 156.2, 157.6, 175.0; HRMS (FAB) *m*/*z* calcd for $C_{39}H_{41}N_2O_7$ ($MH^+$) 649.2908, found 649.2921.

**(3*R*,4*R*)-4-[*N*-(*tert*-Butoxycarbonyl)amino]-5-(4-methoxyphenyl)-3-methylpent-1-en-3-ol (12a).** To a stirred solution of Boc-D-Phe-NMe(OMe) **11** (1.43 g, 4.23 mmol) in THF (35 mL) was added dropwise a solution of MeMgCl in THF (1.9 M, 6.7 mL, 12.7 mmol) at −78 °C under argon, and the mixture was stirred for 1.5 h at −78 °C. The reaction was quenched with saturated citric acid at −78 °C, and the whole was extracted with EtOAc. The extract was washed successively with saturated citric acid, brine, saturated $NaHCO_3$, and brine and dried over $MgSO_4$. Concentration under reduced pressure gave a crude ketone, which was used immediately in the next step without further purification. To a stirred suspension of anhydrous $CeCl_3$ (3.13 g, 12.7 mmol) and the above ketone in THF (30 mL) was added dropwise a solution of vinylmagnesium bromide in THF (1.3 M, 9.8 mL, 12.7 mmol) at 0 °C under argon. After 3 h, the reaction was quenched with saturated citric acid at −78 °C. The mixture was concentrated under reduced pressure and extracted with EtOAc. The extract was washed successively with saturated citric acid, brine, saturated $NaHCO_3$, and brine and dried over $Na_2SO_4$. Concentration under reduced pressure followed by flash chromatography over silica

gel with *n*-hexane–AcOEt (4:1) and recrystallization with *n*-hexane–AcOEt (10:1) gave the title compound **12a** (650 mg, 2.02 mmol, 48% yield) as white solids: mp 94–96 °C; $[\alpha]_D^{22}$ +78.2 (*c* 0.98, $CHCl_3$); IR (neat) 3436 (NH), 1691 (C=O); $^1$H NMR (500 MHz, $CDCl_3$) $\delta$ 1.28–1.37 (m, 12H), 2.50–2.60 (m, 1H), 2.90 (s, 1H), 3.04 (dd, *J* = 14.3, 3.4 Hz, 1H), 3.64–3.71 (m, 1H), 3.77 (s, 3H), 4.52 (d, *J* = 8.0 Hz, 1H), 5.15 (d, *J* = 10.3 Hz, 1H), 5.34 (d, *J* = 17.2 Hz, 1H), 5.98 (dd, *J* = 17.2, 10.3 Hz, 1H), 6.81 (d, *J* = 8.6 Hz, 2H), 7.09 (d, *J* = 8.6 Hz, 2H); $^{13}$C NMR (125 MHz, $CDCl_3$) $\delta$ 24.7, 28.2 (3C), 34.6, 55.3, 60.1, 75.7, 79.5, 113.3, 113.8 (2C), 130.0 (2C), 130.8, 142.8, 156.5, 158.1. Anal. Calcd for $C_{18}H_{27}NO_4$: C, 67.26; H, 8.47; N, 4.36. Found: C, 67.23; H, 8.49; N, 4.42.

**(4*R*,5*R*)-*N*-(*tert*-Butoxycarbonyl)-5-ethenyl-4-(4-methoxybenzyl)-5-methyl-1,3-oxazolidin-2-one (13a).** To a stirred suspension of NaH (1.64 g, 41.1 mmol) in THF (20 mL) was added dropwise a solution of the known allyl alcohol **12a** (3.30 g, 10.3 mmol) in THF (80 mL) at 0 °C under argon, and the mixture was heated under reflux for 1 h and stirred for 30 min at room temperature. $(Boc)_2O$ (4.50 g, 20.6 mmol) was added to the mixture at 0 °C, and the mixture was stirred for 2 h with warming to room temperature. The mixture was poured into water at 0 °C, and the whole was extracted with EtOAc. The extract was washed successively with water and brine and dried over $Na_2SO_4$. Concentration under reduced pressure followed by flash chromatography over silica gel with *n*-hexane–EtOAc (6:1) gave the title compound **13a** (3.58 g, 10.3 mmol, quantitative) as white solids: mp 117–118 °C; $[\alpha]_D^{22}$ +82.3 (*c* 1.02, $CHCl_3$); IR (neat) 1798 (C=O), 1714 (C=O); $^1$H NMR (500 MHz, $CDCl_3$) $\delta$ 1.40 (s, 3H), 1.43 (s, 9H), 2.92 (dd, *J* = 14.3, 8.6 Hz, 1H), 3.06 (dd, *J* = 14.3, 5.7 Hz, 1H), 3.79 (s, 3H), 4.31 (dd, *J* = 8.6, 5.7 Hz, 1H), 5.16 (d, *J* = 10.9 Hz, 1H), 5.34 (d, *J* = 17.2 Hz, 1H), 5.76 (dd, *J* = 17.2, 10.9 Hz, 1H), 6.85 (d, *J* = 8.6 Hz, 2H), 7.15 (d, *J* = 8.6 Hz, 2H); $^{13}$C NMR (125 MHz, $CDCl_3$) $\delta$ 20.6, 27.8 (3C), 35.1, 55.2, 63.2, 82.1, 83.6, 114.2 (2C), 114.5, 128.5, 130.1 (2C), 139.5, 149.3, 151.4, 158.5. Anal. Calcd for $C_{19}H_{25}NO_5$: C, 65.69; H, 7.25; N, 4.03. Found: C, 65.40; H, 7.37; N, 4.03.

***tert*-Butyl (*E*)-3-[(4*R*,5*R*)-*N*-(*tert*-Butoxycarbonyl)-4-(4-methoxybenzyl)-5-methyl-1,3-oxazolidin-2-on-5-yl]prop-2-enoate (15a).** Ozone gas was bubbled into a stirred solution of the oxazolidin-2-one **13a** (211 mg, 0.61 mmol) in EtOAc (10 mL) at −78 °C until a blue color persisted. To the solution was added dimethyl sulfide (890 μL, 12.2 mmol) at −78 °C, and the mixture was stirred for 0.5 h at −78 °C. The mixture was dried over $Na_2SO_4$ and concentrated under reduced pressure to give the corresponding aldehyde, which was used for the next reaction without further purification. To a stirred suspension of LiCl (52.0 mg, 1.22 mmol) in MeCN (4.0 mL) were added *tert*-butyl diethylphosphonoacetate (380 μL, 1.22 mmol) and $(i\text{-}Pr)_2NEt$ (213 μL, 1.22 mmol) successively at 0 °C under argon. After 30 min, the above aldehyde in MeCN (2.0 mL) was added to the mixture at 0 °C, and the stirring was continued for 3.5 h. The reaction was quenched by addition of saturated $NH_4Cl$. After concentration under reduced pressure, the residue was extracted with EtOAc. The extract was washed with saturated citric acid, brine, saturated $NaHCO_3$, and brine and dried over $Na_2SO_4$. Concentration under reduced pressure followed by flash chromatography over silica gel with *n*-hexane–EtOAc (4:1) gave the title compound **15a** (152 mg, 0.34 mmol, 56% yield) as white solids: mp 140–141 °C; $[\alpha]_D^{26}$ +92.8 (*c* 0.99, $CHCl_3$); IR (neat) 1800 (C=O), 1714 (C=O); $^1$H NMR (500 MHz, $CDCl_3$) $\delta$ 1.42 (s, 3H), 1.47 (s, 18H), 2.94 (dd, *J* = 14.3, 9.2 Hz, 1H), 3.12 (dd, *J* = 14.3, 4.6 Hz, 1H), 3.80 (s, 3H), 4.37 (dd, *J* = 9.2, 4.6 Hz, 1H), 6.00 (d, *J* = 16.0 Hz, 1H), 6.63 (d, *J* = 16.0 Hz, 1H), 6.86 (d, *J* = 8.0 Hz, 2H), 7.15 (d, *J* = 8.0 Hz, 2H); $^{13}$C NMR (125 MHz, $CDCl_3$) $\delta$ 20.5, 27.8 (3C), 28.0 (3C), 34.9, 55.2, 62.8, 81.2, 81.3, 84.2, 114.3 (2C), 122.6, 128.0, 130.0 (2C), 146.1, 149.0, 150.9, 158.6, 165.0. Anal. Calcd for $C_{24}H_{33}NO_7$: C, 64.41; H, 7.43; N, 3.13. Found: C, 64.48; H, 7.23; N, 3.10.

***tert*-Butyl (2*R*,5*R*,3*E*)-5-[*N*-(*tert*-Butoxycarbonyl)amino]-2-(3-hydroxypropyl)-6-(4-methoxyphenyl)-4-methylhex-3-enoate (17a).** To a solution of the TBS ether **16a** (52.6 mg, 0.091 mmol) in MeCN–$H_2O$ (1:1, 2.0 mL) was added aqueous $H_2SiF_6$ (3.28 M, 28 μL, 0.091 mmol) at room temperature, and the mixture was stirred for 14 h. The reaction was quenched by addition of saturated $NH_4Cl$. After concentration under reduced pressure, the residue was extracted with EtOAc. The extract was washed with saturated $NH_4Cl$, brine, saturated $NaHCO_3$, and brine and dried over $Na_2SO_4$. Concentration under reduced pressure followed by flash chromatography over silica gel with *n*-hexane–EtOAc (1:1) gave the title compound **17a** (21.7 mg, 0.047 mmol, 51% yield) as a colorless oil: $[\alpha]_D^{25}$ −37.3 (*c* 1.03, $CHCl_3$); IR (neat) 1699 (C=O); $^1$H NMR (500 MHz, $CDCl_3$) $\delta$ 1.28–1.34 (m, 3H), 1.37–1.41 (m, 10H), 1.42 (s, 9H), 1.62–1.70 (m, 4H), 2.76 (d, *J* = 6.9 Hz, 2H), 3.03–3.12 (m, 1H), 3.51 (t, *J* = 6.9 Hz, 2H), 3.77 (s, 3H), 4.09–4.31 (m, 1H), 4.64 (d, *J* = 8.0 Hz, 1H), 5.16 (d, *J* = 9.2 Hz, 1H), 6.80 (d, *J* = 8.6 Hz, 2H), 7.05 (d, *J* = 8.6 Hz, 2H); $^{13}$C NMR (125 MHz, $CDCl_3$) $\delta$ 14.3, 28.0 (3C), 28.3 (3C), 28.7, 29.9, 38.8, 45.1, 55.2, 58.2, 62.4, 79.3, 80.4, 113.7 (2C), 124.5, 129.8, 130.1 (2C), 136.9, 155.0, 158.1, 173.5; HRMS (FAB) *m*/*z* calcd for $C_{26}H_{42}NO_6$ ($MH^+$) 464.3007, found 464.3010.

***tert*-Butyl (2*R*,5*R*,3*E*)-2-{3-[*N*-[(Benzyloxy)carbonyl]-*N*-[(2-nitrophenyl)sulfonyl]amino]propyl}-5-[*N*-(*tert*-butoxycarbonyl)amino]-6-(4-methoxyphenyl)-4-methylhex-3-enoate (18a).** To a solution of the alcohol **17a** (21.7 mg, 0.047 mmol), $PPh_3$ (24.6 mg, 0.094 mmol), and NsNH(Cbz) (33.0 mg, 0.094 mmol) in THF (0.47 mL) was added DEAD in toluene (2.2 M, 43 μL, 0.094 mmol) at 0 °C under argon, and the mixture was stirred at the same temperature overnight. Concentration under reduced pressure followed by flash chromatography over silica gel with *n*-hexane–EtOAc (3:1) gave the title compound **18a** (22.4 mg, 0.029 mmol, 61% yield) as a yellow oil: $[\alpha]_D^{25}$ −24.0 (*c* 1.02, $CHCl_3$); IR (neat) 1726 (C=O); $^1$H NMR (500 MHz, $CDCl_3$) $\delta$ 1.38 (s, 9H), 1.40–1.48 (m, 10H), 1.57–1.78 (m, 6H), 2.69–2.85 (m, 2H), 3.06–3.18 (m, 1H), 3.77 (s, 3H), 3.80 (t, *J* = 7.4 Hz, 2H), 4.12–4.28 (m, 1H), 4.50–4.67 (m, 1H), 5.11 (s, 2H), 5.19 (d, *J* = 9.7 Hz, 1H), 6.80 (d, *J* = 8.6 Hz, 2H), 7.06 (d, *J* = 8.6 Hz, 2H), 7.17–7.25 (m, 2H), 7.29–7.40 (m, 3H), 7.41–7.51 (m, 1H), 7.61–7.76 (m, 2H), 8.10 (d, *J* = 8.0 Hz, 1H); $^{13}$C NMR (125 MHz, $CDCl_3$) $\delta$ 14.3, 27.4, 27.9 (3C), 28.3 (3C), 29.4, 39.0, 45.0, 47.9, 55.2, 58.0, 69.3, 79.1, 80.4, 113.7 (2C), 124.2, 124.3, 128.5 (2C), 128.6 (2C), 128.7, 129.8, 130.1 (2C), 131.5, 132.8, 134.09, 134.11, 134.2, 137.5, 147.7, 151.6, 155.0, 158.1, 173.0; HRMS (FAB) *m*/*z* calcd for $C_{40}H_{52}N_3O_{11}S$ ($MH^+$) 782.3317, found 782.3319.

**(4*R*,5*S*)-5-Acetyl-*N*-(*tert*-butoxycarbonyl)-4-(4-methoxybenzyl)-5-methyl-1,3-oxazolidin-2-one (14).** Ozone gas was bubbled into a stirred solution of the oxazolidin-2-one **13b** (1.20 g, 3.32 mmol) in EtOAc (40 mL) at −78 °C until a blue color persisted. To the solution was added dimethyl sulfide (2.4 mL, 33.2 mmol) at −78 °C, and the mixture was stirred for 15 min at −78 °C. Concentration under reduced pressure followed by flash chromatography over silica gel with *n*-hexane–EtOAc (2:1) gave the title compound **14** (1.19 g, 3.28 mmol, 99% yield) as colorless crystals: mp 91–92 °C; $[\alpha]_D^{26}$ +48.0 (*c* 1.02, $CHCl_3$); IR (neat) 1817 (C=O), 1725 (C=O); $^1$H NMR (500 MHz, $CDCl_3$) $\delta$ 1.35 (s, 3H), 1.44 (s, 9H), 2.28 (s, 3H), 2.93 (dd, *J* = 14.9, 8.6 Hz, 1H), 3.05 (dd, *J* = 14.3, 5.2 Hz, 1H), 3.79 (s, 3H), 4.86 (dd, *J* = 8.6, 5.2 Hz, 1H), 6.85 (d, *J* = 8.6 Hz, 2H), 7.16 (d, *J* = 8.6 Hz, 2H); $^{13}$C NMR (125 MHz, $CDCl_3$) $\delta$ 17.6, 24.8, 27.8 (3C), 34.8, 55.2, 60.0, 84.3, 86.5, 114.3 (2C), 127.7, 130.0 (2C), 148.4, 150.4, 158.6, 207.8. Anal. Calcd for $C_{19}H_{25}NO_6$: C, 62.80; H, 6.93; N, 3.85. Found: C, 62.68; H, 6.80; N, 3.89.

***tert*-Butyl (*E*)-3-[(4*R*,5*R*)-*N*-(*tert*-Butoxycarbonyl)-4-(4-methoxybenzyl)-5-methyl-1,3-oxazolidin-2-on-5-yl]but-2-enoate (15b).** The ketone **14** (490 mg, 1.35 mmol) and $Ph_3P{=}CHCO_2$-*t*-Bu (1.11 g, 2.97 mmol) were dissolved in toluene (6.0 mL), and the mixture was gently refluxed for 10 h. Concentration under reduced pressure followed by flash chromatography over silica gel with *n*-hexane–EtOAc (3:1) gave the title compound **15b** (621 mg, 1.35 mmol, quantitative) as colorless crystals: mp 174–175 °C; $[\alpha]_D^{26}$ +76.7 (*c* 1.00, $CHCl_3$); IR (neat) 1813 (C=O), 1714 (C=O); $^1$H NMR (500 MHz, $CDCl_3$) $\delta$ 1.41 (s, 3H), 1.46 (s, 9H), 1.49 (s, 9H), 1.91 (d, *J* = 1.2 Hz, 3H), 2.94 (dd, *J* = 14.3, 9.2 Hz, 1H), 3.12 (dd, *J* = 14.3, 4.6 Hz, 1H), 3.80 (s, 3H), 4.42 (dd, *J* = 9.2, 4.6 Hz, 1H), 5.95 (d, *J* = 1.2 Hz, 1H), 6.87 (d, *J* = 8.6 Hz, 2H), 7.18 (d, *J* = 8.6 Hz, 2H); $^{13}$C NMR (125 MHz, $CDCl_3$) $\delta$ 14.7, 20.2, 27.9 (3C), 28.1 (3C), 35.3, 55.2,

61.5, 80.5, 84.2, 84.4, 114.3 (2C), 117.1, 128.1, 130.1 (2C), 149.0, 150.6, 153.9, 158.6, 165.7. Anal. Calcd for $C_{25}H_{35}NO_7$: C, 65.06; H, 7.64; N, 3.03. Found: C, 64.97; H, 7.71; N, 3.07.

***tert*-Butyl (*Z*)-3-[(4*R*,5*R*)-*N*-(*tert*-Butoxycarbonyl)-4-(4-methoxybenzyl)-5-methyl-1,3-oxazolidin-2-on-5-yl]but-2-enoate (21).** To a solution of diisopropylamine (41.0 μL, 0.29 mmol) in THF (0.29 mL) at −78 °C was added dropwise *n*-BuLi in *n*-hexane (1.65 M, 0.18 mL, 0.29 mmol). After the mixture was stirred at 0 °C for 30 min, a solution of $TMSCH_2CO_2$-*t*-Bu (66.0 μL, 0.30 mmol) in THF (0.19 mL) was added dropwise at −78 °C. After the mixture was stirred at −78 °C for 2 h, a solution of ketone **14** (21.0 mg, 0.058 mmol) in THF (0.19 mL) was added dropwise. The resulting mixture was stirred at −78 °C for 4 h. The reaction was quenched by addition of saturated $NH_4Cl$ at −78 °C. The whole mixture was stirred at room temperature for 15 min, extracted with $Et_2O$, and dried over $MgSO_4$. Concentration under reduced pressure followed by flash chromatography over silica gel with *n*-hexane−EtOAc (3:1) gave an *E*/*Z* mixture of the title compound **21** and **15b** (14.2 mg, 0.031 mmol, 53% yield, **15b**/**21** = 3/2) as a clear oil. Data for compound **21** (purified by preparative HPLC): colorless oil; $[\alpha]_D^{25}$ −115.7 (*c* 1.01, $CHCl_3$); IR (neat) 1818 (C=O), 1705 (C=O); $^1$H NMR (500 MHz, DMSO-$d_6$) δ 1.16 (s, 9H), 1.52 (s, 9H), 1.73 (s, 3H), 1.94 (d, *J* = 1.7 Hz, 3H), 2.66 (dd, *J* = 13.7, 10.3 Hz, 1H), 3.30 (dd, *J* = 13.7, 3.4 Hz, 1H), 3.77 (s, 3H), 4.76 (dd, *J* = 10.3, 3.4 Hz, 1H), 5.74 (d, *J* = 1.7 Hz, 1H), 6.82 (d, *J* = 8.6 Hz, 2H), 7.14 (d, *J* = 8.6 Hz, 2H); $^{13}$C NMR (125 MHz, DMSO-$d_6$) δ 19.2, 22.7, 27.4 (3C), 28.1 (3C), 36.2, 55.2, 65.2, 80.7, 82.9, 85.9, 114.0 (2C), 119.0, 129.0, 130.7 (2C), 148.7, 151.6, 158.5, 160.8, 164.7; HRMS (FAB) *m*/*z* calcd for $C_{25}H_{36}NO_7$ ($MH^+$) 462.2486 found 462.2486.

**Peptide Synthesis.** The protected linear peptides **28a**−**c** were constructed by Fmoc-based solid-phase synthesis on H-Gly-(2-Cl)Trt resin (0.66 mmol/g, 152 mg, 0.10 mmol). The Pbf group for Arg was employed for side chain protection. Fmoc-protected amino acids (0.30 mmol) were coupled by using *N*,*N*′-diisopropylcarbodiimide (DIC) (46.4 μL, 0.3 mmol) and HOBt·$H_2O$ (45.9 mg, 0.3 mmol) in DMF. Coupling of dipeptide isostere **10**, **20a**, or **20b** (0.30 mmol) was carried out with DIC (46.4 μL, 0.3 mmol) and HOAt (40.8 mg, 0.30 mmol). Completion of each coupling reaction was ascertained using the Kaiser ninhydrin test. The Fmoc protecting group was removed by treating the resin with 20% piperidine in DMF.

By use of a procedure identical with that described for the preparation of the protected linear peptide, **28d** was obtained from H-Gly-(2-Cl)Trt resin (0.80 mmol/g, 125 mg, 0.10 mmol) using dipeptide isostere **26** (0.30 mmol).

**Cyclo(D-Tyr-ψ[(*E*)-CH=CH]-Arg-Arg-Nal-Gly-)·2TFA (31a).** The resulting protected peptide resin **28a** (275 mg) was subjected to hexafluoro-2-propanol (HFIP)−$CH_2Cl_2$ (2:8, 15 mL) treatment at room temperature for 2 h. After filtration of the residual resin, the filtrate was concentrated under reduced pressure to give a crude linear peptide, **29a**. To a mixture of the linear peptide and $NaHCO_3$ (42.0 mg, 0.500 mmol) in DMF (40 mL) was added diphenylphosphoryl azide (DPPA; 53.9 μL, 0.250 mmol) at −40 °C. The mixture was stirred for 40 h with warming to room temperature and then filtered. The filtrate was concentrated under reduced pressure, followed by flash chromatography over silica gel with $CHCl_3$−MeOH (90:10) to give the protected cyclic peptide **30a**. The peptide **30a** was treated with 1 M TMSOTf−thioanisole in TFA (3 mL) at room temperature for 3 h. Concentration under reduced pressure gave an oily residue, which was used immediately in the next step without purification. To a solution of the crude mixture in DMF (2 mL) were added $(i\text{-Pr})_2$NEt (261 μL, 1.50 mmol) and 1*H*-pyrazole-1-carboxamidine hydrochloride (73.3 mg, 0.500 mmol), and the mixture was stirred at room temperature for 2 days. After concentration under reduced pressure, purification by preparative HPLC gave the bistrifluoroacetate of the title cyclic peptide **31a** (20.4 mg, 0.0217 mmol, 22% yield based on H-Gly-(2-Cl)Trt resin) as a colorless freeze-dried powder: $[\alpha]_D^{28}$ −43.4 (*c* 0.133, DMSO); $^1$H NMR (500 MHz, DMSO-$d_6$) δ 1.25−1.50 (m, 5H), 1.52−1.70 (m, 3H), 2.58 (d, *J* = 7.6 Hz, 2H), 2.74 (ddd, *J* = 8.2, 8.2, 7.6 Hz, 1H), 2.94−3.15 (m, 6H), 3.29 (dd, *J* = 15.8, 5.5 Hz, 1H), 3.66 (dd, *J* = 15.8, 6.9 Hz, 1H), 4.14 (ddd, *J* = 8.9, 8.2, 8.2 Hz, 1H), 4.32−4.41 (m, 1H), 4.53 (ddd, *J* = 7.6, 7.6, 6.9 Hz, 1H), 5.39 (ddd, *J* = 15.1, 8.9, 1.4 Hz, 1H), 5.55 (dd, *J* = 15.1, 4.1 Hz, 1H), 6.62 (d, *J* = 8.3 Hz, 2H), 6.93 (d, *J* = 8.3 Hz, 2H), 7.02 (d, *J* = 8.3 Hz, 1H), 7.30 (dd, *J* = 8.3, 2.1 Hz, 1H), 7.42−7.50 (m, 2H), 7.50−7.57 (m, 2H), 7.61 (s, 1H), 7.76 (d, *J* = 8.9 Hz, 1H), 7.79−7.87 (m, 4H), 8.35 (dd, *J* = 6.9, 5.5 Hz, 1H), 9.15 (s, 1H); $^{13}$C NMR (125 MHz, DMSO-$d_6$) δ 25.3, 26.3, 27.9, 28.4, 29.0, 38.1, 40.1 (overlapped with DMSO peaks), 40.3, 43.5, 50.3, 51.5, 54.3, 54.5, 115.0 (2C), 125.5, 126.0, 127.4, 127.4, 127.5, 127.6, 127.66, 127.75, 128.0, 130.1 (2C), 131.9, 132.8, 132.9, 134.8, 155.6, 156.72, 156.75, 167.6, 170.6, 171.5, 172.2; HRMS (FAB) *m*/*z* calcd for $C_{37}H_{49}N_{10}O_5$ ($MH^+$) 713.3882, found 713.3881.

**Cyclo(D-Tyr-ψ[-$CH_2$-$CH_2$]-Arg-Arg-Nal-Gly-)·2TFA (31e).** The cyclic pseudopeptide **31a** (2.64 mg, 0.0281 mmol) was treated with Pd/$BaSO_4$ (59.5 mg, 0.0281 mmol) in MeOH (300 μL) under a $H_2$ atmosphere at room temperature for 36 h. After filtration and concentration under reduced pressure, purification by preparative HPLC gave the bistrifluoroacetate of the title peptide **31e** (0.874 mg, 0.00927 mmol, 33% yield) as a colorless freeze-dried powder: $[\alpha]_D^{29}$ −31.7 (*c* 0.0933, DMSO); $^1$H NMR (500 MHz, DMSO-$d_6$) δ 1.08−1.53 (m, 10H), 1.61−1.79 (m, 2H), 1.91−2.04 (m, 1H), 2.35 (dd, *J* = 13.2, 7.4 Hz, 1H), 2.46−2.58 (m, 1H, overlapped with DMSO peak), 2.95−3.10 (m, 4H), 3.14 (dd, *J* = 13.7, 9.7 Hz, 1H), 3.24 (dd, *J* = 13.7, 4.6 Hz, 1H), 3.44−3.48 (m, 1H), 3.61−3.72 (m, 1H), 3.75−3.84 (m, 1H), 3.84−3.93 (m, 1H), 4.42−4.52 (m, 1H), 6.45 (d, *J* = 9.7 Hz, 1H), 6.62 (d, *J* = 8.0 Hz, 2H), 6.89 (d, *J* = 8.0 Hz, 2H), 7.41−7.56 (m, 5H), 7.76 (s, 1H), 7.82−7.90 (m, 3H), 8.10 (d, *J* = 7.4 Hz, 1H), 8.13−8.21 (m, 1H), 8.26−8.36 (m, 1H), 9.14 (s, 1H); $^{13}$C NMR (125 MHz, DMSO-$d_6$) δ 25.4, 26.5, 27.0, 29.0, 29.3, 31.2, 36.4, 40.2, 40.4, 41.2, 42.5, 46.9, 50.4, 53.7, 56.1, 115.0 (2C), 125.5, 126.1, 127.2, 127.4, 127.47, 127.55, 127.8, 128.7, 129.9 (2C), 131.8, 133.0, 135.6, 155.5, 156.68, 156.70, 168.0, 170.7, 172.6, 174.8; HRMS (FAB) *m*/*z* calcd for $C_{37}H_{51}N_{10}O_5$ ($MH^+$) 715.4038, found 715.4046.

**[$^{125}$I]SDF-1 Binding and Displacement.** Membrane extracts were prepared from HEK293 cell lines expressing CXCR4. For ligand binding, 50 μL of the inhibitor, 25 μL of [$^{125}$I]SDF-1α (0.3 nM, Perkin-Elmer Life Sciences), and 25 μL of the membrane/bead mixture [7.5 μg of membrane/well, 0.5 mg of PVT WGA beads (Amersham)/well] in assay buffer (25 mM HEPES, pH 7.4, 1 mM $CaCl_2$, 5 mM $MgCl_2$, 140 mM NaCl, 250 mM sucrose, 0.5% BSA) were incubated in the wells of an Optiplate plate (Perkin-Elmer Life Sciences) at room temperature for 1 h. The bound radioactivity was counted for 1 min/well in a TopCount (Packard). The inhibitory activity of the test compounds was determined on the basis of the inhibition of [$^{125}$I]SDF-1 binding to the receptors ($IC_{50}$, triplicate experiments, Table 1).

**NMR Spectroscopy.** The peptide sample was dissolved in DMSO-$d_6$ at 5 mM. $^1$H NMR spectra of the peptides were recorded at 300 K. The assignment of the proton resonance was achieved by use of $^1$H−$^1$H COSY spectra. COSY spectra were composed of 2048 complex points in the $F_2$ dimension and 256 complex points, which were zero-filled to yield a final data matrix of 2048 × 512 points. $^3J(H^N,H^\alpha)$ coupling constants were measured from one-dimensional spectra. The mixing time for NOESY experiments was set at 200 ms. NOESY spectra were composed of 1024 complex points in the $F_2$ dimension and 512 complex points, which were zero-filled to yield a final data matrix of 1024 × 1024 points, with 32 scans per $t_1$ increment. The cross-peak intensities were classified on the basis of the number of contour lines.

**Structural Calculations.** The structure calculations were performed by MacroModel using the MMFFs. Pseudoatoms were defined for the $CH_3$ protons on the alkene of **31b**−**d**, methylene protons of D-Tyr[1], D/L-Arg[2], L-Arg[3], and L-Nal[4], and aromatic protons of D-Tyr[1], the prochiralities of which were not identified from $^1$H NMR data. The dihedral φ angle constraints were calculated on the basis of the Karplus equation: $^3J(H^N,H^\alpha) = 6.7\cos^2\theta - 1.3\cos\theta + 1.5$. Lower and upper angle errors were set to 15°. The NOESY spectrum with a mixing time of 200 ms was used for the estimation of the distance restraints between protons. The NOE intensities were classified into three categories (strong, medium, and weak) on the basis of the number of contour lines in the cross-peaks to define the

upper limit distance restraints (2.7, 3.5, and 5.0 Å, respectively). The upper limit restraints were increased by 1.0 Å for the involved pseudoatoms except the aromatic protons, for which the restraints were increased by 2.0 Å. Lower bounds between nonbonded atoms were set to their van der Waals radii (1.8 Å). A total of 100 000 random structures were generated by molecular dynamic simulation starting with any initial structure in water; the structures matched with the restraints from the NMR data were then selected. The structure in the lowest potential energy was defined as the most stable structure in solution.

**Docking of Peptidomimetics to CXCR4.** Initial structures of **31a–c**, **31d-A**, and **31d-B** were built by energy minimization of NMR-based structures described above. The resulting models were incorporated into CXCR4, and the water molecules of the crystal structure of CXCR4 bound to CVX15 (PDB code 3OE0) were manually input as appropriate. After that, the structures of peptidomimetics were minimized in the receptor structure in MOE using MMFF94s and a distance-dependent dielectric constant of 1 with a 10 Å cutoff distance. The steepest descent algorithm was used for the minimization, followed by the conjugate gradient method. The maximum iterations of each run were set to 100 steps, and the root-mean-square (rms) gradient value of 0.01 was set for the criteria of the minimizations. In this calculation, the backbone atoms of the receptor were fixed.

## ■ ASSOCIATED CONTENT

### Supporting Information

Experimental procedures and characterization data for all new compounds. This material is available free of charge via the Internet at http://pubs.acs.org.

## ■ AUTHOR INFORMATION


### Corresponding Author

*Phone: +81-75-753-4551. Fax: +81-75-753-4570. E-mail: soishi@pharm.kyoto-u.ac.jp (S.O.); nfujii@pharm.kyoto-u.ac.jp (N.F.).


### Notes

The authors declare no competing financial interest.

## ■ ACKNOWLEDGMENTS

This work was supported by Grants-in-Aid for Scientific Research and the Targeted Protein Research Program from MEXT and Health and Labor Science Research Grants (Research on HIV/AIDS, Japan). K.K. and K.T. are grateful for JSPS Research Fellowships for Young Scientists.

## ■ ABBREVIATIONS USED

CXCR4, CXC chemokine receptor type 4; HWE reaction, Horner–Wadsworth–Emmons reaction; HIV, human immunodeficiency virus; MMFFs, Merck molecular force field; MOE, Molecular Operating Environment; Nal, 3-(2-naphthyl)alanine; Orn, ornithine; SAR, structure–activity relationship; SDF-1, stromal-cell-derived factor-1

## ■ REFERENCES


(1) Fung, S.; Hruby, V. J. Design of cyclic and other templates for potent and selective peptide α-MSH analogues. *Curr. Opin. Chem. Biol.* **2005**, *9*, 352–358.

(2) Mosberg, H. I.; Hurst, R.; Hruby, V. J.; Gee, K.; Yamaura, H. I.; Galligan., J. J.; Burks, T. F. Bis-penicillamine enkephalins possess highly improved specificity toward δ opioid receptors. *Proc. Natl. Acad. Sci. U.S.A.* **1983**, *80*, 5871–5874.

(3) March, D. R.; Abbenante, G.; Bergman, D. A.; Brinkworth, R. I.; Wickramasinghe, W.; Begun, J.; Martin, J. L.; Fairlie, D. P. Substrate-based cyclic peptidomimetics of Phe-Ile-Val that inhibit HIV-1 protease using a novel enzyme-binding mode. *J. Am. Chem. Soc.* **1996**, *118*, 3375–3379.

(4) Burton, P. S.; Conradi, R. A.; Ho, N. F. H.; Hilgers, A. R.; Borchardt, R. T. How structural features influence the biomembrane permeability of peptides. *J. Pharm. Sci.* **1996**, *85*, 1336–1340.

(5) Rezai, T.; Yu, B.; Millhauser, G. L.; Jacobson, M. P.; Lokey, R. S. Testing the conformational hypothesis of passive membrane permeability using synthetic cyclic peptide diastereomers. *J. Am. Chem. Soc.* **2006**, *128*, 2510–2511.

(6) Kessler, H. Conformation and biological activity of cyclic peptides. *Angew. Chem., Int. Ed. Engl.* **1982**, *21*, 512–523.

(7) Aumailley, M.; Gurrath, M.; Müller, G.; Calvete, J.; Timpl, R.; Kessler, H. Arg-Gly-Asp constrained within cyclic pentapeptides. Strong and selective inhibitors of cell adhesion to vitronectin and laminin fragment P1. *FEBS Lett.* **1991**, *291*, 50–54.

(8) Dechantsreiter, M. A.; Planker, E.; Mathä, B.; Lohof, E.; Hölzemann, G.; Jonczyk, A; Goodman, S. L.; Kessler, H. *N*-Methylated cyclic RGD peptides as highly active and selective $\alpha_v\beta_3$ integrin antagonists. *J. Med. Chem.* **1999**, *42*, 3033–3040.

(9) Haubner, R.; Gratias, R.; Diefenbach, B.; Goodman, S. L.; Jonczyk, A.; Kessler, H. Structural and functional aspects of RGD-containing cyclic pentapeptides as highly potent and selective integrin $\alpha_v\beta_3$ antagonists. *J. Am. Chem. Soc.* **1996**, *118*, 7461–7472.

(10) Keenan, R. M.; Miller, W. H.; Kwon, C.; Ali, F. E.; Callahan, J. F.; Calvo, R. R.; Hwang, S. M.; Kopple, K. D.; Peishoff, C. E.; Samanen, J. M.; Wong, A. S.; Yuan, C. K.; Huffman, W. F. Discovery of potent nonpeptide vitronectin receptor ($\alpha_v\beta_3$) antagonists. *J. Med. Chem.* **1997**, *40*, 2289–2292.

(11) Nicolaou, K. C.; Trujillo, J. I.; Jandeleit, B.; Chibale, K.; Rosenfeld, M.; Diefenbach, B.; Cheresh, D. A.; Goodman, S. L. Design, synthesis and biological evaluation of nonpeptide integrin antagonists. *Bioorg. Med. Chem.* **1998**, *6*, 1185–1208.

(12) Rockwell, A. L.; Rafalski, M.; Pitts, W. J.; Batt, D. G.; Petraitis, J. J.; DeGrado, W. F.; Mousa, S.; Jadhav, P. K. Rapid synthesis of RGD mimetics with isoxazoline scaffolds on solid phase: identification of $\alpha_v\beta_3$ antagonists lead compounds. *Bioorg. Med. Chem. Lett.* **1999**, *9*, 937–942.

(13) Ihara, M.; Noguchi, K.; Saeki, T.; Fukuroda, T.; Tsuchida, S.; Kimura, S.; Fukami, T.; Ishikawa, K.; Nishikibe, M.; Yano, M. Biological profiles of highly potent novel endothelin antagonists selective for the $ET_A$ receptor. *Life Sci.* **1992**, *50*, 247–255.

(14) Kikuchi, T.; Ohtaki, T.; Kawata, A.; Imada, T.; Asami, T.; Masuda, Y.; Sugo, T.; Kusumoto, K.; Kubo, K.; Watanabe, T.; Wakimasu, M.; Fujino, M. Cyclic hexapeptide endothelin receptor antagonists highly potent for both receptor subtypes $ET_A$ and $ET_B$. *Biochem. Biophys. Res. Commun.* **1994**, *200*, 1708–1712.

(15) Iqbal, J.; Sanghi, R.; Das, S. K. Endothelin receptor antagonists: an overview of their synthesis and structure-activity relationship. *Mini-Rev. Med. Chem.* **2005**, *5*, 381–408.

(16) Cardillo, G.; Gentilucci, L.; Tolomelli, A.; Spinosa, R.; Calienni, M.; Qasem, A. R.; Spampinato, S. Synthesis and evaluation of the affinity toward μ-opioid receptors of atypical, lipophilic ligands based on the sequence *c*[-Tyr-Pro-Trp-Phe-Gly-]. *J. Med. Chem.* **2004**, *47*, 5198–5203.

(17) Gentilucci, L.; Squassabia, F.; Demarco, R.; Artali, R.; Cardillo, G.; Tolomelli, A.; Spampinato, S.; Bedini, A. Investigation of the interaction between the atypical agonist c[YpwFG] and MOR. *FEBS J.* **2008**, *275*, 2315–2337.

(18) Veber, D. F.; Freidinger, R. M.; Perlow, D. S.; Paleveda, W. J. Jr.; Holly, F. W.; Strachan, R. G.; Nutt, R. F.; Arison, B. H.; Homnick, C.; Randall, W. C.; Glitzer, M. S.; Saperstein, R.; Hirschmann, R. A potent cyclic hexapeptide analogue of somatostatin. *Nature* **1981**, *292*, 55–58.

(19) Veber, D. F.; Saperstein, R.; Nutt, R. F.; Freidinger, R. M.; Brady, S. F.; Curley, P.; Perlow, D. S.; Paleveda, W. J.; Colton, C. D.; Zacchei, A. G.; Tocco, D. J.; Hoff, D. R.; Vandlen, R. L.; Gerich, J. E.; Hall, L.; Mandarino, L.; Cordes, E. H.; Anderson, P. S.; Hirschmann, R. A super active cyclic hexapeptide analog of somatostatin. *Life Sci.* **1984**, *34*, 1371–1378.

(20) Fujii, N.; Oishi, S.; Hiramatsu, K.; Araki, T.; Ueda, S.; Tamamura, H.; Otaka, A.; Kusano, S.; Terakubo, S.; Nakashima, H.; Broach, J. A.; Trent, J. O.; Wang, Z.; Peiper, S. C. Molecular-size reduction of a potent CXCR4-chemokine antagonist using orthogonal combination of conformation- and sequence-based libraries. *Angew. Chem., Int. Ed.* **2003**, *42*, 3251−3253.
(21) Inokuchi, E.; Oishi, S.; Kubo, T.; Ohno, H.; Shimura, K.; Matsuoka, M.; Fujii, N. Potent CXCR4 antagonists containing amidine type peptide bond isosteres. *ACS Med. Chem. Lett.* **2011**, *2*, 477−480 and references therein.
(22) Ueda, S.; Oishi, S.; Wang, Z.; Araki, T.; Tamamura, H.; Cluzeau, J.; Ohno, H.; Kusano, S.; Nakashima, H.; Trent, J. O.; Peiper, S. C.; Fujii, N. Structure-activity relationships of cyclic peptide-based chemokine receptor CXCR4 antagonists: disclosing the importance of side-chain and backbone functionalities. *J. Med. Chem.* **2007**, *50*, 192−198.
(23) Hann, M. M.; Sammes, P. G.; Kennewell, P. D.; Taylor, J. B. On double bond isosteres of the peptide bond; an enkephalin analogue. *J. Chem. Soc., Chem. Commun.* **1980**, 234−235.
(24) Hann, M. M.; Sammes, P. G.; Kennewell, P. D.; Taylor, J. B. On the double bond isostere of the peptide bond: preparation of an enkephalin analogue. *J. Chem. Soc., Perkin. Trans. 1* **1982**, 307−314.
(25) Christos, T. E.; Arvanitis, A.; Cain, G. A.; Johnson, A. L.; Pottorf, R. S.; Tam, S. W.; Schmidt, W. K. Stable isosteres of neurotensin C-terminal pentapeptides derived by modification of the amide function. *Bioorg. Med. Chem. Lett.* **1993**, *3*, 1035−1040.
(26) Wipf, P.; Henninger, T. C.; Geib, S. J. Methyl- and (triflоromethyl)alkene peptide isosteres: synthesis and evaluation of their potential as $\beta$-turn promoters and peptide mimetics. *J. Org. Chem.* **1998**, *63*, 6088−6089.
(27) Xiao, J.; Weisblum, B.; Wipf, P. Trisubstituted (*E*)-alkene dipeptide isosteres as $\beta$-turn promoters in the gramicidin S cyclodecapeptide scaffold. *Org. Lett.* **2006**, *8*, 4731−4734.
(28) Oishi, S.; Miyamoto, K.; Niida, A.; Yamamoto, M.; Ajito, K.; Tamamura, H.; Otaka, A.; Kuroda, Y.; Asai, A.; Fujii, N. Application of tri- and tetrasubstituted alkene dipeptide mimetics to conformational studies of cyclic RGD peptides. *Tetrahedron* **2006**, *62*, 1416−1424.
(29) Narumi, T.; Tomita, K.; Inokuchi, E.; Kobayashi, K.; Oishi, S.; Ohno, H.; Fujii, N. Diastereoselective synthesis of highly functionalized fluoroalkene dipeptide isosteres and its application to Fmoc-based solid-phase synthesis of a cyclic pentapeptide mimetic. *Tetrahedron* **2008**, *64*, 4332−4346.
(30) Narumi, T.; Hayashi, R.; Tomita, K.; Kobayashi, K.; Tanahara, N.; Ohno, H.; Naito, T.; Kodama, E.; Matsuoka, M.; Oishi, S.; Fujii, N. Synthesis and biological evaluation of selective CXCR4 antagonists containing alkene dipeptide isosteres. *Org. Biomol. Chem.* **2010**, *8*, 616−621.
(31) Ibuka, T.; Habashita, H.; Funakoshi, S.; Fujii, N.; Oguchi, Y.; Uyehara, T.; Yamamoto, Y. Highly selective synthesis of (*E*)-alkene isosteric dipeptides with high optical purity via RCu(CN)Li·$BF_3$ mediated reaction. *Angew. Chem., Int. Ed. Engl.* **1990**, *29*, 801−803.
(32) Oishi, S.; Niida, A.; Kamano, T.; Odagaki, Y.; Tamamura, H.; Otaka, A.; Hamanaka, N.; Fujii, N. Diastereoselective synthesis of $\psi$[(*E*)-CMe=CH]- and $\psi$[(*E*)-CMe=CMe]-type dipeptide isosteres based on organocopper-mediated *anti*-$S_N2'$ reaction. *Org. Lett.* **2002**, *4*, 1055−1058.
(33) Oishi, S.; Niida, A.; Kamano, T.; Miwa, Y.; Taga, T.; Odagaki, Y.; Hamanaka, N.; Yamamoto, M.; Ajito, K.; Tamamura, H.; Otaka, A.; Fujii, N. Regio- and stereoselective ring-opening of chiral 1,3-oxazolidin-2-one derivatives by organocopper reagents provides novel access to di-, tri- and tetra-substituted alkene dipeptide isosteres. *J. Chem. Soc., Perkin Trans. 1* **2002**, 1786−1793.
(34) Ando, K. Highly selective synthesis of *Z*-unsaturated esters by using new Horner−Emmons reagents, ethyl (diarylphosphono)-acetates. *J. Org. Chem.* **1997**, *62*, 1934−1939.
(35) Yu, J. S.; Kleckley, T. S.; Wiemer, D. F. Synthesis of farnesol isomers via a modified Wittig procedure. *Org. Lett.* **2005**, *7*, 4803−4806.
(36) Peterson, D. J. A carbonyl olefination reaction using silyl-substituted organometallic compounds. *J. Org. Chem.* **1968**, *33*, 780−784.
(37) Hartzell, S. L.; Sullivan, D. F.; Rathke, M. W. Reaction of lithio *tert*-butyl trimethylsilylacetate with aldehydes and ketones. A synthesis of $\alpha,\beta$-unsaturated esters. *Tetrahedron Lett.* **1974**, *15*, 1403−1406.
(38) Våbenø, J.; Nikiforovich, G. V.; Marshall, G. R. Insight into the binding mode for cyclopentapeptide antagonists of the CXCR4 receptor. *Chem. Biol. Drug Des.* **2006**, *67*, 346−354.
(39) Våbenø, J.; Nikiforovich, G. V.; Marshall, G. R. A minimalistic 3D pharmacophore model for cyclopentapeptide CXCR4 antagonists. *Biopolymers* **2006**, *84*, 459−471.
(40) Demmer, O.; Dijkgraaf, I.; Schumacher, U.; Marinelli, L.; Cosconati, S.; Gourni, E.; Wester, H. J.; Kessler, H. Design, synthesis, and functionalization of dimeric peptides targeting chemokine receptor CXCR4. *J. Med. Chem.* **2011**, *54*, 7648−7662.
(41) Yoshikawa, Y.; Kobayashi, K.; Oishi, S.; Fujii, N.; Furuya, T. Molecular modeling study of cyclic pentapeptide CXCR4 antagonists: new insight into CXCR4-FC131 interactions. *Bioorg. Med. Chem. Lett.* **2012**, *22*, 2146−2150.
(42) Wu, B.; Chien, E. Y. T.; Mol, C. D.; Fenalti, G.; Liu, W.; Katritch, V.; Abagyan, R.; Brooun, A.; Wells, P.; Bi, F. C.; Hamel, D. J.; Kuhn, P.; Handel, T. M.; Cherezov, V.; Stevens, R. C. Structure of the CXCR4 chemokine GPCR with small-molecule and cyclic peptide antagonists. *Science* **2010**, *330*, 1066−1071.
(43) Molecular Operating Environment (MOE), Chemical Computing Group Inc., Montreal, QC, Canada.

研究成果の刊行に関する一覧表

研究分担者　国立感染症研究所エイズ研究センター　村上　努

雑誌

| 発表者氏名 | 論文タイトル名 | 発表誌名 | 巻号 | ページ | 出版年 |
|---|---|---|---|---|---|
| Narumi T, Komoriya M, Hashimoto C, Wu H, Nomura W, Suzuki S, Tanaka T, Chiba J, Yamamoto N, Murakami T, Tamamura H. | Conjugation of cell-penetrating peptides leads to identification of anti-HIV peptides from matrix proteins. | Bioorg. Med. Chem. | 20 | 1468-1474 | 2012 |
| Tanaka T, Narumi T, Ozaki T, Sohma A, Ohashi N, Hashimoto C, Itotani K, Nomura W, Murakami T, Yamamoto N, Tamamura H. | Azamacrocyclic-metal complexes as CXCR4 antagonists.Azamacrocyclic-metal complexes as CXCR4 antagonists. | Chem. Med. Chem. | 6 | 834-839 | 2011 |
| Yanagita H, Urano E, Mastumoto K, Ichikawa R, Takaesu Y, Ogata M, Murakami T, Wu H, Chiba J, Komano J, Hosino T. | Structural and biochemical study on the inhibitory activity of derivatives of 5-nitro-furan-2-carboxylic acid for RNase H function of HIV-1 reverse transcriptase. | Bioorg. Med. Chem. | 19 | 816-825 | 2011 |

Bioorganic & Medicinal Chemistry 20 (2012) 1468–1474

Contents lists available at SciVerse ScienceDirect

Bioorganic & Medicinal Chemistry

journal homepage: www.elsevier.com/locate/bmc

# Conjugation of cell-penetrating peptides leads to identification of anti-HIV peptides from matrix proteins

Tetsuo Narumi [a], Mao Komoriya [a], Chie Hashimoto [a], Honggui Wu [b,c], Wataru Nomura [a], Shintaro Suzuki [a], Tomohiro Tanaka [a], Joe Chiba [c], Naoki Yamamoto [d], Tsutomu Murakami [b,*], Hirokazu Tamamura [a,*]

[a] Institute of Biomaterials and Bioengineering, Tokyo Medical and Dental University, Chiyoda-ku, Tokyo 101-0062, Japan
[b] AIDS Research Center, National Institute of Infectious Diseases, Shinjuku-ku, Tokyo 162-8640, Japan
[c] Department of Biological Science Technology, Tokyo University of Science, Noda, Chiba 278-8510, Japan
[d] Yong Loo Lin School of Medicine, National University of Singapore, Singapore 117597, Singapore

ARTICLE INFO

*Article history:*
Received 6 December 2011
Revised 24 December 2011
Accepted 24 December 2011
Available online 2 January 2012

*Keywords:*
Matrix protein
Octa-arginyl group
Overlapping peptide
Anti-HIV

ABSTRACT

Compounds which inhibit the HIV-1 replication cycle have been found amongst fragment peptides derived from an HIV-1 matrix (MA) protein. Overlapping peptide libraries covering the whole sequence of MA were designed and constructed with the addition of an octa-arginyl group to increase their cell membrane permeability. Imaging experiments with fluorescent-labeled peptides demonstrated these peptides with an octa-arginyl group can penetrate cell membranes. The fusion of an octa-arginyl group was proven to be an efficient way to find active peptides in cells such as HIV-inhibitory peptides.



## 1. Introduction

Several anti-retroviral drugs beyond reverse transcriptase inhibitors, including effective protease inhibitors[1] and integrase inhibitors[2,3] are currently available to treat human immunodeficiency virus type 1 (HIV-1) infected individuals. We have also developed several anti-HIV agents such as coreceptor CXCR4 antagonists,[4–7] CD4 mimics,[8–10] fusion inhibitors[11] and integrase inhibitors.[12,13] However, the emergence of viral strains with multi-drug resistance (MDR), which accompanies the development of any antiviral drug, has encouraged a search for new types of anti-HIV-1 drugs with different inhibitory mechanisms.

Matrix (MA) proteins are essential for assembly of the virion shell. MA is a component of the Gag precursor protein, Pr55Gag, and is located within the viral membrane.[14,15] It has been reported that MA-derived peptides such as MA(47–59) inhibit infection by HIV,[16] and that MA-derived peptides such as MA(31–45) and MA(41–55) show anti-HIV activity.[17] In addition, Morikawa et al. report that MA(61–75) and MA(71–85) inhibit MA dimerization, a necessary step in the formation of the virion shell.[18] However, the question of whether the above MA peptides can penetrate cell membranes was not addressed in these reports. We speculate that to achieve antiviral activity it is essential that the MA-derived peptides penetrate the cell membrane and function intracellularly. In this paper, we report our design and construction of an overlapping library of fragment peptides derived from the MA protein with a cell membrane permeable signal. Our aim is the discovery of potent lead compounds, which demonstrate HIV inhibitory activity inside the host cells.

## 2. Materials and methods

### 2.1. Peptide synthesis

MA-derived fragments and an octa-arginyl ($R_8$) peptide were synthesized by stepwise elongation techniques of Fmoc-protected amino acids on a Rink amide resin. Coupling reactions were performed using 5.0 equiv of Fmoc-protected amino acid, 5.0 equiv of diisopropylcarbodiimide and 5.0 equiv of 1-hydroxybenzotriazole monohydrate. $Ac_2O$–pyridine (1/1, v/v) for 20 min was used to acetylate the N-terminus of MA-derived fragments, with the exception of fragment 1. Chloroactylation of the N-terminus of the $R_8$ peptide, was achieved with 40 equiv of chloroacetic acid, 40 equiv of diisopropylcarbodiimide and 40 equiv of 1-hydroxybenzotriazole monohydrate, treated for 1 h. Cleavage of peptides from resin and side chain deprotection were carried out by stirring for 1.5 h with a mixture of TFA, thioanisole, ethanedithiol, *m*-cresol

* Corresponding authors. Tel.: +81 3 5285 1111; fax: +81 3 5285 5037 (T.M.); tel.: +81 3 5280 8036; fax: +81 3 5280 8039 (H.M.).
*E-mail addresses:* tmura@nih.go.jp (T. Murakami), tamamura.mr@tmd.ac.jp (H. Tamamura).

0968-0896/$ - see front matter © 2011 Elsevier Ltd. All rights reserved.
doi:10.1016/j.bmc.2011.12.055

and triisopropylsilane (8.15/0.75/0.75/0.25/0.25/0.1, v/v). After removal of the resins by filtration, the filtrate was concentrated under reduced pressure, and crude peptides were precipitated in cooled diethyl ether. All crude peptides were purified by RP-HPLC and identified by ESI-TOFMS. In the conjugation of the $R_8$ peptide (or iodoacetamide), the peptide (or iodoacetamide) solution in 0.1 M phosphate buffer, pH 7.8 was added to MA fragments which were synthesized as described above. The reaction mixture was stirred at room temperature under nitrogen. After 24 h (or 1 h for the conjugation of iodoacetamide), purification was performed by RP-HPLC. The purified peptides were identified by ESI-TOF MS and lyophilized. Purities of all final compounds were confirmed to be >95% by analytical HPLC. Detailed data are provided in Supplementary data.

### 2.2. Anti-HIV-1 assay

Anti-HIV-1 (NL4-3 or NL(AD8)) activity was determined by measurement of the protection against HIV-1-induced cytopathogenicity in MT-4 cells or PM1/CCR5 cells. Various concentrations of test peptide solutions were added to HIV-1 infected MT-4 or PM1/CCR5 cells at multiplicity of infection (MOI) of 0.001 and placed in wells of a 96-well microplate. After 5 day incubation at 37 °C in a $CO_2$ incubator, the number of viable cells was determined using the 3-(4,5-dimethylthiazol-2-yl)-2,5-diphenyltetrazolium bromide (MTT) method. The anti-HIV-1 (JR-CSF) activity was also determined by measuring capsid p24 antigen concentrations of the culture supernatant in the infected cultures by a commercially available ELISA assay (ZeptoMetrix Corp., Buffalo, NY).

### 2.3. CD spectroscopy

CD spectra were recorded on a JASCO J-720 spectropolarimeter at 25 °C. The measurements were performed using a 0.1 cm path length cuvette at a 0.1 nm spectral resolution. Each spectrum represents the average of 10 scans, and the scan rate was 50 nm/min. The concentrations of samples 8L and 9L were 28.2 and 64.7 μM, respectively, in PBS buffer (pH 7.4).

### 2.4. Fluorescent imaging of cell-penetrating MA peptides

Cells were seeded on 35 mm glass-bottom dish ($2 \times 10^5$ cells/dish for HeLa and A549, $1 \times 10^5$ cells/dish for CHO-K1) one day before the experiments. The cells were cultured in DMEM/10% FBS/Penicillin–Streptomycin for HeLa and A549, or Ham's F12/10% FBS/Penicillin–Streptomycin for CHO-K1 at 37 °C/5% $CO_2$. Before the addition of MA peptides, cells were washed with Hanks' balanced salt solutions (HBSS) once. Peptides were added at 5 μM and further cultured for 30 min at 37 °C/5% $CO_2$. After incubation, cells were washed three times with HBSS and observed under a confocal laser-scanning microscopy (Zeiss LSM510).

## 3. Results and discussion

An overlapping peptide library spanning the whole sequence of the MA domain, p17, of NL4-3, the Gag precursor Pr55 of HIV-1 was designed. The full sequence of MA consists of 132 amino acid residues. In the peptide library, the MA sequence was divided from the N-terminus in 15-residue segments with an overlap of 5

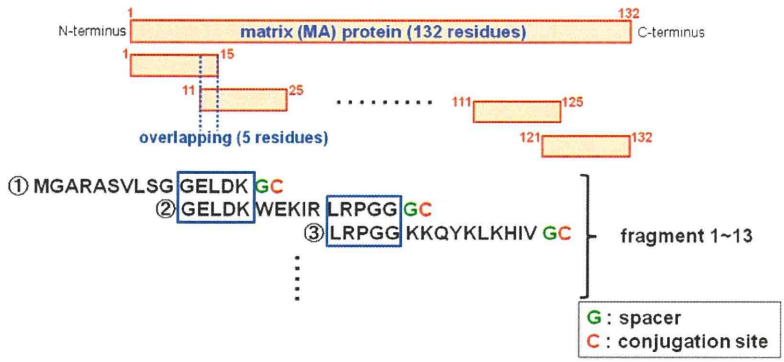


| fragment number | sequence |
|---|---|
| 1 | H-MGARASVLSGGELDKGC-$NH_2$ |
| 2 | $CH_3CO$-GELDKWEKIRLRPGGGC-$NH_2$ |
| 3 | $CH_3CO$-LRPGGKKQYKLKHIVGC-$NH_2$ |
| 4 | $CH_3CO$-LKHIVWASRELERFAGC-$NH_2$ |
| 5 | $CH_3CO$-LERFAVNPGLLETSEGC-$NH_2$ |
| 6 | $CH_3CO$-LETSEGSRQILGQLQGC-$NH_2$ |
| 7 | $CH_3CO$-LGQLQPSLQTGSEELGC-$NH_2$ |
| 8 | $CH_3CO$-GSEELRSLYNTIAVLGC-$NH_2$ |
| 9 | $CH_3CO$-TIAVLYSVHQRIDVKGC-$NH_2$ |
| 10 | $CH_3CO$-RIDVKDTKEALDKIEGC-$NH_2$ |
| 11 | $CH_3CO$-LDKIEEEQNKSKKKAGC-$NH_2$ |
| 12 | $CH_3CO$-SKKKAQQAAADTGNNGC-$NH_2$ |
| 13 | $CH_3CO$-DTGNNSQVSQNYGC-$NH_2$ |

**Figure 1.** The construction of MA-based overlapping peptide library.

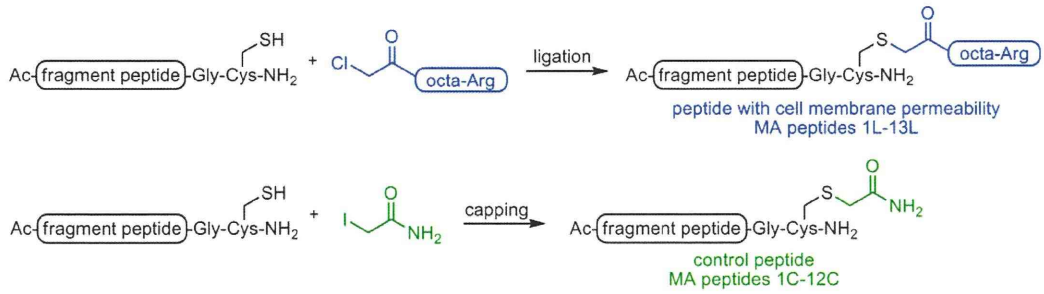


**Figure 2.** The design of MA peptides with cell membrane permeability (upper) and their control peptides (lower).

residues to preserve secondary structures (Fig. 1). Cys residues of the original MA sequence were changed into Ser residues because of the facility of peptide synthesis. Thirteen MA fragment peptides (1–13) were designed with the addition of Gly as a spacer and Cys as a conjugation site at the C-terminus. To impart cell membrane permeability to these peptides, the N-terminal chloroacetyl group of an octa-arginyl ($R_8$) peptide[19] was conjugated to the side-chain thiol group of the Cys residue of the above peptides. This resulted in the MA peptides 1L–13L (Fig. 2). $R_8$ is a cell membrane permeable motif and its fusion with parent peptides is known to produce bioactive peptides with no significant adverse properties.[12,13,20–24] In addition, the $R_8$-fusion can increase the solubility of MA

**Table 1**
Anti-HIV activity and cytotoxicity of control MA peptides

| MA peptide | MT-4 cell | PM1/CCR5 cell | | MT-4 cell |
|---|---|---|---|---|
| | NL4-3 (MTT assay) $EC_{50}$[a] (μM) | NL(AD8) (MTT assay) $EC_{50}$[a] (μM) | JR-CSF (p24 ELISA) $EC_{50}$[a] (μM) | (MTT assay) $CC_{50}$[b] (μM) |
| 1C | >50 | ND | ND | >50 |
| 2C | 17 ± 1.4 | 1.0 | ND | >50 |
| 3C | >50 | ND | ND | >50 |
| 4C | No inhibition at 12.5 μM | ND | ND | 14 |
| 5C | >50 | ND | ND | >50 |
| 6C | 37 ± 12 | 24% inhibition at 6.25 μM | 25% inhibition at 50 μM | >50 |
| 7C | >50 | ND | ND | >50 |
| 8C | >50 | ND | ND | >50 |
| 9C | 29 ± 1.4 | 13 | 8.1 | >50 |
| 10C | No inhibition at 12.5 μM | ND | ND | 17 |
| 11C | >50 | ND | ND | >50 |
| 12C | >50 | ND | ND | >50 |
| 14C | >50 | ND | ND | >50 |
| AZT | 0.020 | 0.459 | 0.17 | >100 |
| SCH-D | ND | 0.026 | 0.0014 | ND |

X4-HIV-1 (NL4-3 strain)-induced cytopathogenicity in MT-4 cells and R5-HIV-1 (NL(AD8) strain)-induced cytopathogenicity in PM1/CCR5 cells evaluated by the MTT assay, and inhibitory activity against R5-HIV-1 (JR-CSF strain)-induced cytopathogenicity in PM1/CCR5 cells evaluated by the p24 ELISA assay.

[a] $EC_{50}$ values are the concentrations for 50% protection from HIV-1-induced cytopathogenicity in MT-4 cells.

[b] $CC_{50}$ values are the concentrations for 50% reduction of the viability of MT-4 cells. All data are the mean values from at least three independent experiments. ND: not determined.

**Table 2**
Anti-HIV activity and cytotoxicity of MA peptides with cell membrane permeability

| MA peptide | MT-4 cell | PM1/CCR5 cell | | MT-4 cell |
|---|---|---|---|---|
| | NL4-3(MTT assay) $EC_{50}$ (μM) | NL(AD8)(MTT assay) $EC_{50}$ (μM) | JR-CSF(p24 ELISA) $EC_{50}$ (μM) | (MTT assay) $CC_{50}$ (μM) |
| 1L | 30 | 30 | 40 | >50 |
| 2L | 21 ± 4.2 | >31 | ND | 32 ± 4.2 |
| 3L | no inhibition at 25 μM | ND | ND | 36 |
| 4L | no inhibition at 3.13 μM | ND | ND | 3.7 |
| 5L | 40 | 42% inhibition at 50 μM | 42 | >50 |
| 6L | 40 ± 8.9 | 49% inhibition at 50 μM | 31 | >50 |
| 7L | 35 ± 1.5 | 37% inhibition at 50 μM | 35% inhibition at 50 μM | >50 |
| 8L | 2.3 ± 0.3 | 5.8 | 7.8 | 9.0 ± 2.4 |
| 9L | 2.1 ± 0.5 | 0.43 | 0.58 | 5.7 ± 2.1 |
| 10L | 43 ± 8.5 | 42% inhibitionat 50 μM | 27 | >50 |
| 11L | 18 ± 3.0 | 17% inhibition at 25 μM | 23 | >50 |
| 12L | 41 ± 5.5 | 30% inhibition at 25 μM | 27 | >50 |
| 13L | 20 ± 2.1 | 0.43 | 11 | >50 |
| 14L | no inhibition at 25 μM | ND | ND | 36 |
| AZT | 0.020 | 0.459 | 0.17 | >100 |
| SCH-D | ND | 0.026 | 0.0014 | ND |

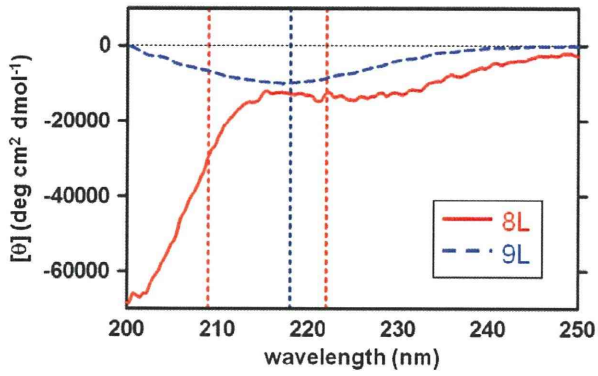


**Figure 3.** CD spectra of MA peptides 8L (28 μM) and 9L (65 μM) in PBS buffer, pH 7.4 at 25 °C.

peptides whose hydrophobicity is relatively limited. On the other hand, to develop control peptides lacking cell membrane permeability, iodoacetamide was conjugated to the thiol group of the Cys residue to prepare MA peptides 1C–12C (Fig. 2). MA peptide 13C was not synthesized because MA fragment 13 is insoluble in PBS buffer.

The anti-HIV activity of MA peptides 1L–13L and MA peptides 1C–12C, was evaluated. Inhibitory activity against T-cell line-tropic (X4-) HIV-1 (NL4-3 strain)-induced cytopathogenicity in MT-4 cells and against macrophage-tropic (R5-) HIV-1 (NL(AD8) strain)-induced cytopathogenicity in PM1/CCR5 cells was assessed by the 3-[4,5-dimethylthiazol-2-yl]-2,5-diphenyltetrazolium bromide (MTT) assay, and inhibitory activity against R5-HIV-1 (JR-CSF strain) replication in PM1/CCR5 cells was determined by the p24 ELISA assay. The results are shown in Tables 1 and 2. The control MA peptides 6C and 9C showed slight anti-HIV activity against NL4-3, NL(AD8) and JR-CSF strains, and 2C showed high anti-HIV activity against NL4-3 and NL(AD8) strains, but the other control MA peptides showed no significant anti-HIV activity. 2C showed significant anti-HIV activity against both X4-HIV-1 and R5-HIV-1 strains, suggesting that this region of the MA domain is relevant with Gag localization to the plasma membrane (PM)[25] and that 2C might inhibit competitively the interaction between MA and PM. On the other hand, the MA peptides with the exception of 3L and 4L, showed moderate to potent anti-HIV activity against all three strains. These peptides expressed almost the same level of anti-HIV activity against both X4-HIV-1 and R5-HIV-1 strains. The MA peptides 8L and 9L in particular, showed significant anti-HIV activity. These results suggest that MA peptides achieve entry into target cells as a result of the addition of $R_8$, and inhibit viral replication within the cells. The adjacent peptides 8L and 9L possess an overlapping sequence TIAVL. Such peptides exhibited relatively high cytotoxicity and the MA peptide 4L showed the highest cytotoxicity although it did not show any significant anti-HIV activity. The control MA peptides 1C–12C were relatively weakly cytotoxic. The MA peptides 8C and 9C exhibited no significant cytotoxicity, although the addition of $R_8$, giving 8L and 9L, caused a remarkable increase in cytotoxicity. This suggests that the octa-arginyl ($R_8$) sequence is correlated with the

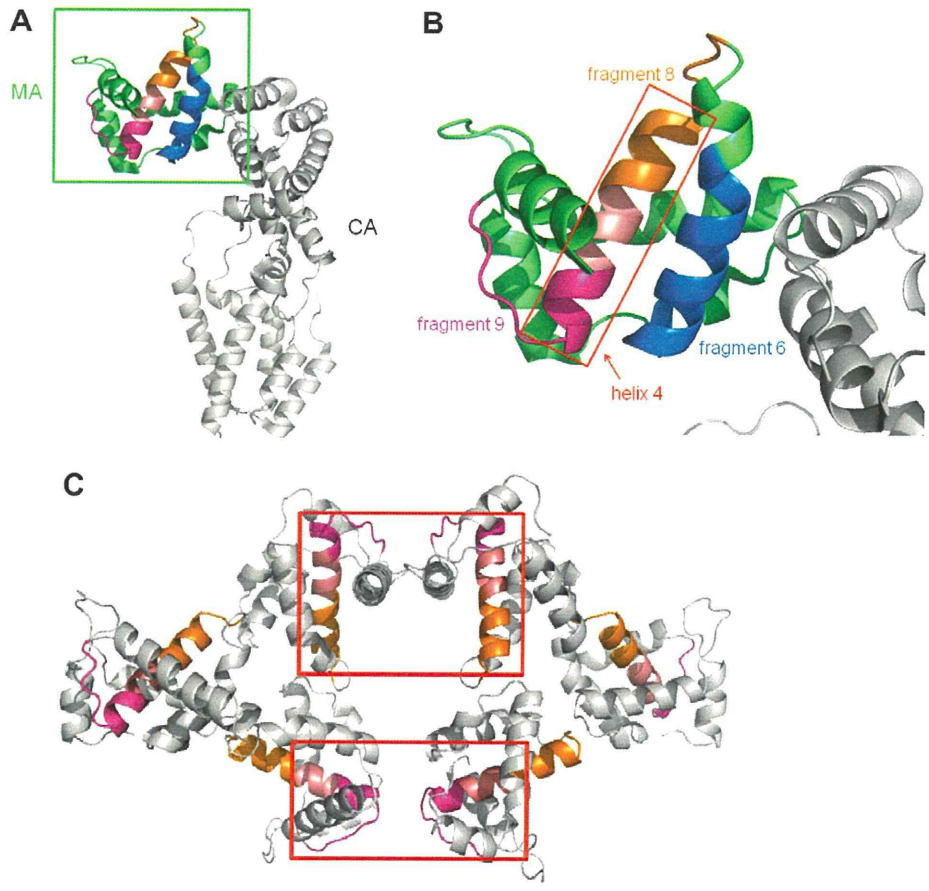


**Figure 4.** (A) The complete structure of MA and CA proteins (PDB ID: 2gol). (B) The enlarged structure of the highlighted region of (A). (C) The structure of an MA hexamer. Red-colored squares show interfaces between two MA trimers (PDB ID: 1hiw). Orange- and pink-colored helical ribbons represent fragments 8 and 9, respectively.

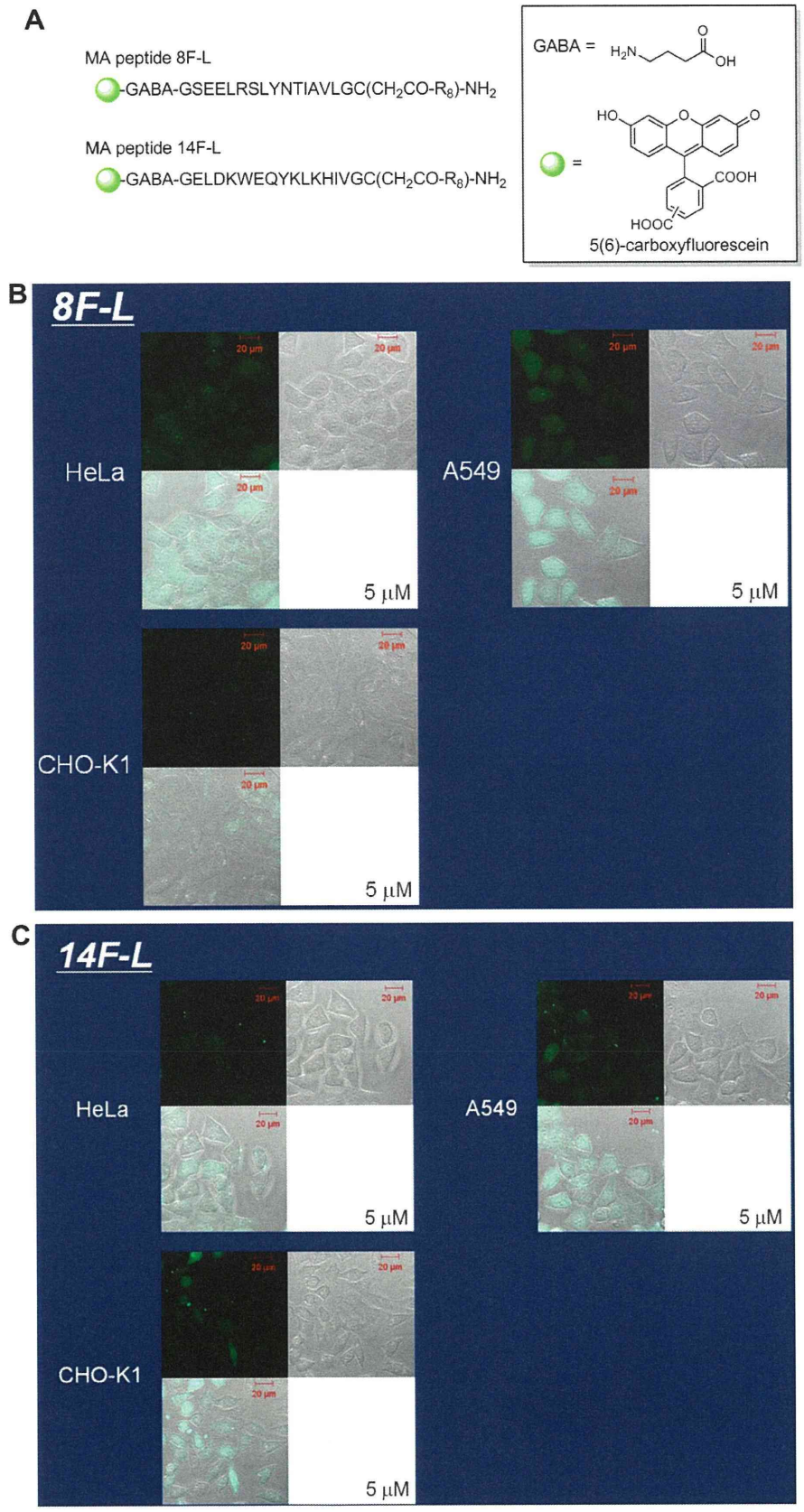


**Figure 5.** (A) The structures of fluorophore-labeled MA peptides 8F–L and 14F–L. (B) The fluorescent imaging of live cells HeLa, A549 and CHO-K1 by 8F–L. (C) The fluorescent imaging of live cells HeLa, A549 and CHO-K1 by 14F–L.

expression of cytotoxicity and in future, a different effective strategy for cell penetration may be advisable.

In the present assay, the control MA peptides 6C and 9C, which cover MA(51–65) and MA(81–95), respectively, showed significant anti-HIV activity. This is consistent with the previous studies, in which MA(41–55), MA(47–59) and MA(71–85) showed anti-HIV or dimerization inhibitory activity as discussed above.[16–18] These peptides have no $R_8$ sequence and thus cannot penetrate cell membranes. They exhibit inhibitory activity on the surface of cells, not intracellularly.

The structures of MA peptides 8L and 9L, dissolved in PBS buffer (2.7 mM KCl, 137 mM NaCl, 1.47 mM $KH_2PO_4$, 9.59 mM $Na_2HPO_4$) at pH 7.4, were determined by CD spectroscopy (Fig. 3). When peptides form α-helical structures, minima can be observed at approximately 207 and 222 nm in their CD spectra. The amino acid residues covering fragments 8 and 9 corresponding to 8L and 9L are located in an α-helical region (helix 4) of the parent MA protein (Fig. 4), and peptides 8L and 9L were presumed to have an α-helical conformation.[26–28] However, the CD spectra shown in Figure 3, suggest that these peptides lack any characteristic secondary structure. This is because the 15-mer peptide derived from MA is not sufficiently long to form a secondary structure even though Gly, Cys and octa-Arg are attached to their C-terminus. Analysis of the CD spectra suggests MA fragment peptides need a longer sequence in order to form a secondary structure. The CD spectra of the control MA peptides 8C and 9C were not determined because the aqueous solubility of these peptides is inadequate.

Fluorescent imaging of live cells was used to evaluate the cell membrane permeability of the MA peptides 8L and 14L, which showed high and zero significant anti-HIV activity, respectively. The MA fragment 14 is a hybrid of the fragments 2 and 3, and the MA peptides 14L and 14C, which are based on the conjugation of the N-terminal chloroacetyl group of an $R_8$ peptide and iodoacetamide to the thiol group of the Cys residue, respectively (Supplementary data), are control peptides lacking significant anti-HIV activity (Tables 1 and 2). These peptides were labeled with 5(6)-carboxyfluorescein via a GABA linker at the N-terminus to produce 8F–L and 14F–L (Fig. 5A). The fluorophore-labeled peptides 8F–L and 14F–L were incubated with live cells of HeLa, A549 and CHO-K1, and the imaging was analyzed by a fluorescence microscope (Fig. 5B and C). A549 cells are human lung adenocarcinomic human alveolar basal epithelial cells.[29] Similar penetration of both peptides 8F–L and 14F–L into these cells was observed. Even peptides without significant anti-HIV activity can penetrate cell membranes. The penetration efficiency of both peptides into A549 was relatively high and into HeLa was low. In CHO-K1 the penetration efficiency of 8F–L is relatively low, but that of 14F–L is high. These imaging data confirm that the MA peptides with the $R_8$ sequence can penetrate cell membranes and suggest that MA peptides such as 8L and 9L should be able to inhibit HIV replication inside cells.

## 4. Conclusions

Several HIV-1 inhibitory fragment peptides were identified through the screening of an overlapping peptide library derived from the MA protein. Judging by the imaging experiments, peptides possessing the $R_8$ group can penetrate cell membranes and might exhibit their function intracellularly thus inhibiting HIV replication.

Two possible explanations for the inhibitory activity of these MA fragment peptides can be envisaged: (1) The fragment peptides might attack an MA protein and inhibit the assembly of MA proteins. (2) These peptides might attack a cellular protein and inhibit its interaction with MA. Further studies to elucidate detailed action mechanisms and identify the targets of these peptides will be performed in future. The technique of addition of the $R_8$ group to peptides enabled us to screen library peptides that function within cells. Thus, the design of an overlapping peptide library of fragment peptides derived from a parent protein with a cell membrane permeable signal is a useful and efficient strategy for finding potent cell-penetrating lead compounds.

In the present study, the MA peptides 8L and 9L were shown to inhibit HIV-1 replication with submicromolar to micromolar $EC_{50}$ values in cells using the MT-4 assay (NL4-3 and NL(AD8) strains) and the p24 ELISA assay (JR-CSF strain). Our findings suggest that these peptides could serve as lead compounds for the discovery of novel anti-HIV agents. Amino acid residues covering fragments 8 and 9 corresponding to 8L and 9L are located in the exterior surface of MA, and in particular in the interface between two MA trimers (Fig. 4C).[26–28] The interaction of two MA trimers leads to the formation of an MA hexamer, which is the MA assembly with physiological significance. Thus, the region covering fragments 8 and 9 is critical to oligomerization of MA proteins. This suggests that MA peptides 8L and 9L might inhibit the MA oligomerization through competitive binding to the parent MA, and that more potent peptides or peptidomimetic HIV inhibitors could result from studies on the mechanism of action of these MA peptides and identification of the interaction sites. Taken together, some seeds for anti-HIV agents are inherent in MA proteins, including inhibitors of the interaction with PM such as the MA peptide 2C.

## Acknowledgements

This work was supported in part by Grant-in-Aid for Scientific Research from the Ministry of Education, Culture, Sports, Science, and Technology of Japan, and Health and Labour Sciences Research Grants from Japanese Ministry of Health, Labor, and Welfare. C.H. and T.T. were supported by JSPS Research Fellowships for Young Scientists. The authors thank Ms. M. Kawamata, National Institute of Infectious Diseases, for her assistance in the anti-HIV assay. We also thank Dr. Y. Maeda, Kumamoto University, for providing PM1/CCR5 cells, and Mr. S. Kumakura, Kureha Corporation, for providing SCH-D, respectively.

## Supplementary data

Supplementary data associated with this article can be found, in the online version, at doi:10.1016/j.bmc.2011.12.055.

## References and notes

1. Ghosh, A. K.; Dawson, Z. L.; Mitsuya, H. *Bioorg. Med. Chem.* **2007**, *15*, 7576.
2. Cahn, P.; Sued, O. *Lancet* **2007**, *369*, 1235.
3. Grinsztejn, B.; Nguyen, B.-Y.; Katlama, C.; Gatell, J. M.; Lazzarin, A.; Vittecoq, D.; Gonzalez, C. J.; Chen, J.; Harvey, C. M.; Isaacs, R. D. *Lancet* **2007**, *369*, 1261.
4. Tamamura, H.; Xu, Y.; Hattori, T.; Zhang, X.; Arakaki, R.; Kanbara, K.; Omagari, A.; Otaka, A.; Ibuka, T.; Yamamoto, N.; Nakashima, H.; Fujii, N. *Biochem. Biophys. Res. Commun.* **1998**, *253*, 877.
5. Fujii, N.; Oishi, S.; Hiramatsu, K.; Araki, T.; Ueda, S.; Tamamura, H.; Otaka, A.; Kusano, S.; Terakubo, S.; Nakashima, H.; Broach, J. A.; Trent, J. O.; Wang, Z.; Peiper, S. C. *Angew. Chem., Int. Ed.* **2003**, *42*, 3251.
6. Tamamura, H.; Hiramatsu, K.; Mizumoto, M.; Ueda, S.; Kusano, S.; Terakubo, S.; Akamatsu, M.; Yamamoto, N.; Trent, J. O.; Wang, Z.; Peiper, S. C.; Nakashima, H.; Otaka, A.; Fujii, N. *Org. Biomol. Chem.* **2003**, *1*, 3663.
7. Tanaka, T.; Nomura, W.; Narumi, T.; Masuda, A.; Tamamura, H. *J. Am. Chem. Soc.* **2010**, *132*, 15899.
8. Yamada, Y.; Ochiai, C.; Yoshimura, K.; Tanaka, T.; Ohashi, N.; Narumi, T.; Nomura, W.; Harada, S.; Matsushita, S.; Tamamura, H. *Bioorg. Med. Chem. Lett.* **2010**, *20*, 354.
9. Narumi, T.; Ochiai, C.; Yoshimura, K.; Harada, S.; Tanaka, T.; Nomura, W.; Arai, H.; Ozaki, T.; Ohashi, N.; Matsushita, S.; Tamamura, H. *Bioorg. Med. Chem. Lett.* **2010**, *20*, 5853.
10. Yoshimura, K.; Harada, S.; Shibata, J.; Hatada, M.; Yamada, Y.; Ochiai, C.; Tamamura, H.; Matsushita, S. *J. Virol.* **2010**, *84*, 7558.

11. Otaka, A.; Nakamura, M.; Nameki, D.; Kodama, E.; Uchiyama, S.; Nakamura, S.; Nakano, H.; Tamamura, H.; Kobayashi, Y.; Matsuoka, M.; Fujii, N. *Angew. Chem., Int. Ed.* **2002**, *41*, 2937.
12. Suzuki, S.; Urano, E.; Hashimoto, C.; Tsutsumi, H.; Nakahara, T.; Tanaka, T.; Nakanishi, Y.; Maddali, K.; Han, Y.; Hamatake, M.; Miyauchi, K.; Pommier, Y.; Beutler, J. A.; Sugiura, W.; Fuji, H.; Hoshino, T.; Itotani, K.; Nomura, W.; Narumi, T.; Yamamoto, N.; Komano, J. A. *J. Med. Chem.* **2010**, *53*, 5356.
13. Suzuki, S.; Maddali, K.; Hashimoto, C.; Urano, E.; Ohashi, N.; Tanaka, T.; Ozaki, T.; Arai, H.; Tsutsumi, H.; Narumi, T.; Nomura, W.; Yamamoto, N.; Pommier, Y.; Komano, J. A.; Tamamura, H. *Bioorg. Med. Chem.* **2010**, *18*, 6771.
14. Freed, E. O. *Virology* **1998**, *251*, 1.
15. Bukrinskaya, A. *Virus Res.* **2007**, *124*, 1.
16. Niedrig, M.; Gelderblom, H. R.; Pauli, G.; März, J.; Bickhard, H.; Wolf, H.; Modrow, S. *J. Gen. Virol.* **1994**, *75*, 1469.
17. Cannon, P. M.; Matthews, S.; Clark, N.; Byles, E. D.; Iourin, O.; Hockley, D. J.; Kingsman, S. M.; Kingsman, A. J. *J. Virol.* **1997**, *71*, 3474.
18. Morikawa, Y.; Kishi, T.; Zhang, W. H.; Nermut, M. V.; Hockley, D. J.; Jones, I. M. *J. Virol.* **1995**, *69*, 4519.
19. Suzuki, T.; Futaki, S.; Niwa, M.; Tanaka, S.; Ueda, K.; Sugiura, Y. *J. Biol. Chem.* **2002**, *277*, 2437.
20. Wender, P. A.; Mitchell, D. J.; Pattabiraman, K.; Pelkey, E. T.; Steinman, L.; Rothbard, J. B. *Proc. Natl. Acad. Sci. U.S.A.* **2000**, *97*, 13003.
21. Matsushita, M.; Tomizawa, K.; Moriwaki, A.; Li, S. T.; Terada, H.; Matsui, H. *J. Neurosci.* **2001**, *21*, 6000.
22. Takenobu, T.; Tomizawa, K.; Matsushita, M.; Li, S. T.; Moriwaki, A.; Lu, Y. F.; Matsui, H. *Mol. Cancer Ther.* **2002**, *1*, 1043.
23. Wu, H. Y.; Tomizawa, K.; Matsushita, M.; Lu, Y. F.; Li, S. T.; Matsui, H. *Neurosci. Res.* **2003**, *47*, 131.
24. Rothbard, J. B.; Garlington, S.; Lin, Q.; Kirschberg, T.; Kreider, E.; McGrane, P. L.; Wender, P. A.; Khavari, P. A. *Nat. Med.* **2000**, *6*, 1253.
25. Ono, A. *J. Virol.* **2004**, *78*, 1552.
26. Rao, Z.; Belyaev, A. S.; Fry, E.; Roy, P.; Jones, I. M.; Stuart, D. I. *Nature* **1995**, *378*, 743.
27. Hill, C. P.; Worthylake, D.; Bancroft, D. P.; Christensen, A. M.; Sundquist, W. I. *Proc. Natl. Acad. Sci. U.S.A.* **1996**, *93*, 3099.
28. Kelly, B. N.; Howard, B. R.; Wang, H.; Robinson, H.; Sundquist, W. I.; Hill, C. P. *Biochemistry* **2006**, *45*, 11257.
29. Murdoch, C.; Monk, P. N.; Finn, A. *Immunology* **1999**, *98*, 36.

CHEMMEDCHEM

DOI: 10.1002/cmdc.201000548

# Azamacrocyclic Metal Complexes as CXCR4 Antagonists

Tomohiro Tanaka,[a] Tetsuo Narumi,*[a] Taro Ozaki,[a] Akira Sohma,[a] Nami Ohashi,[a] Chie Hashimoto,[a] Kyoko Itotani,[a] Wataru Nomura,[a] Tsutomu Murakami,[b] Naoki Yamamoto,[b, c] and Hirokazu Tamamura*[a]

The chemokine receptor CXCR4 is a member of the seven transmembrane GPCR family, which is implicated in multiple diseases, including HIV infection, cancers, and rheumatoid arthritis. Low-molecular-weight nonpeptidic compounds, including AMD3100 and various pyridyl macrocyclic zinc(II) complexes, have been identified as selective antagonists of CXCR4. In the present study, structure–activity relationship studies were performed by combining the common structural features of alkylamino and pyridiyl macrocyclic antagonists. Several new zinc(II) or copper(II) complexes demonstrated potent anti-HIV activity, strong CXCR4-binding activity, and significant inhibitory activity against $Ca^{2+}$ mobilization induced by CXCL12 stimulation. These results may prove useful in the design of novel CXCR4 antagonists, and the compounds described could potentially be developed as therapeutics against CXCR4-relevant diseases or chemical probes to study the biological activity of CXCR4.

## Introduction

The chemokine receptor CXCR4, which transduces signals of its endogenous ligand, CXCL12/stromal cell-derived factor-1 (SDF-1),[1–4] is classified as a member of the seven transmembrane GPCR family, and plays a physiological role via its interaction with CXCL12 in chemotaxis,[5] angiogenesis,[6,7] and neurogenesis[8,9] in embryonic stages. CXCR4 is, however, relevant to multiple diseases including HIV infection/AIDS,[10,11] metastasis of several types of cancer,[12–14] leukemia cell progression,[15,16] and rheumatoid arthritis (RA),[17,18] and is considered an attractive drug target to combat these diseases. Thus, inhibitors targeting CXCR4 are expected to be useful for drug discovery.

Several CXCR4 antagonists have been reported,[19–35] including our discovery of the highly potent CXCR4 antagonist T140, a 14-mer peptide with a disulfide bridge, its smaller derivative, the 5-mer cyclic peptide FC131, and several other potent analogues.[19,24–26,28–30] Clinical development of these peptidic antagonists could be pursued using specific administration strategies involving biodegradable microcapsules.[14,36] However, herein we focus on novel nonpeptidic low-molecular-weight CXCR4 antagonists. To date, AMD3100 (**1**),[20,22] Dpa-Zn complex (**2**),[37] KRH-1636,[27] and other compounds[31–35] have been developed in this and other laboratories as low-molecular-weight nonpeptidic CXCR4 antagonists. The present study reports structure–activity relationship studies based on the combination of common structural motifs, such as xylene scaffolds and cationic moieties that are present in the aforementioned compounds.

## Results and Discussion

In order to determine spatially suitable positioning of cationic moieties, *p*- and *m*-xylenes were utilized as spacers. Cationic moieties such as bis(pyridin-2-ylmethyl)amine (dipicolylamine), 1,4,7,10-tetraazacyclododecane (cyclen), and 1,4,8,11-tetraazacyclotetradecane (cyclam) were introduced as $R^1$ and $R^2$ (Figure 1). This combination of $R^1$, $R^2$, and spacer groups led to the design and synthesis of compounds **12–31**.

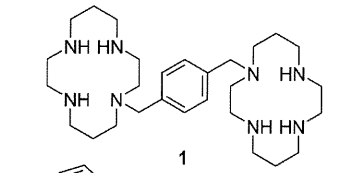


1

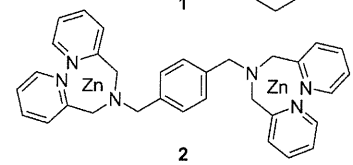


2

The CXCR4 binding activity of synthetic compounds was assessed based on the inhibition of [$^{125}$I]CXCL12 binding to Jurkat cells, which express CXCR4.[38] The percent inhibition of all compounds at 1 μM is shown in Table 1. Seven compounds (**16**, **17**, **20–22**, **28**, and **29**, Table 1) resulted in greater than 87% inhibition. The high activity of **16** is consistent with re-

[a] T. Tanaka, Dr. T. Narumi, T. Ozaki, A. Sohma, N. Ohashi, C. Hashimoto, K. Itotani, Dr. W. Nomura, Prof. H. Tamamura
Institute of Biomaterials and Bioengineering
Tokyo Medical and Dental University
2-3-10 Kandasurugadai, Chiyoda-ku, Tokyo 101-0062 (Japan)
Fax: (+81) 3-5280-8039
E-mail: tamamura.mr@tmd.ac.jp

[b] Dr. T. Murakami, Prof. N. Yamamoto
AIDS Research Center, National Institute of Infectious Diseases
1-23-1 Toyama, Shinjuku-ku, Tokyo 162-8640 (Japan)

[c] Prof. N. Yamamoto
Department of Microbiology, Yong Loo Lin School of Medicine
National University of Singapore, Singapore 117597 (Singapore)

Supporting information for this article is available on the WWW under http://dx.doi.org/10.1002/cmdc.201000548.